The Development of an IrAl Coated SiC-C Functionally Gradient Composite for Oxidation Protection of Graphite and Carbon-Carbon Composites

Final Report to AFOSR(#F49620-92-J-0367)

October 27, 1995

M.R. Richards, A.C. Richards, F.S. Ohuchi
Department of Materials Science and Engineering

and M. Taya
Department of Mechanical Engineering
University of Washington
Seattle, WA 98915

DISCLAIMER NOTICE

THIS DOCUMENT IS BEST QUALITY AVAILABLE. THE COPY FURNISHED TO DTIC CONTAINED A SIGNIFICANT NUMBER OF PAGES WHICH DO NOT REPRODUCE LEGIBLY.

October 27, 1995 Final(7/15/92-7/14/95)

The Development of an IrAl Coated SiC-C Functionally Gradient Composite for Oxidation Protection of Graphite and Carbon-Carbon Composites

AFOSR #F49620-92-J-0367

M.R. Richards, A.C. Richards, M. Taya and F.S. Ohuchi

Department of Mechanical Engineering, and Materials Science and Engineering, University of Washington
Seattle, WA 98195

UW-ME-95-002

Dr. Walter F. Jones
Aerospace Science
US Air Force of Scientific Office
Bolling Air FOrce Base, DC 20332-6448

Unlimited

This report is the final summary for AFOSR project number F49620-92-J-0367. The purpose of this research was to evaluate the oxidation protection afforded to graphite or C/C composites by combining IrAl with SiC-C functionally gradient coatings FGCs. This project involved the design and construction of a novel cold wall levitation chemical vapor deposition (LCVD) reactor capable of producing continuous FGCs, and the modification of an existing physical vapor deposition (PVD) system to allow for codeposition of Ir and Al. The SiC-C FGCs were produced using the $SiCl_4$-C_3H_8-H_2 gas system. By continuously varying the Si to C ratio in the gas stream the composition of the coatings could be precisely controlled and tailored to fit a predetermined compositional profile. IrAl was deposited onto the SiC-C FGC by alternately depositing layers of Ir and Al and reacting them at 700°C, in vacuum, to form IrAl. Analysis of the as reacted film indicated that IrAl had indeed formed, however, a secondary reaction had occurred between the Ir and SiC producing $IrSi_3$ and graphite. Cracking of the IrAl coating was also observed and was attributed to the CTE mismatch between SiC and the IrAl coating. Upon exposure to a high temperature oxidizing flame (<2100°C for 5 min.), the IrAl formed a protective layer of alumina, however, the extensive cracking of the IrAl layer allowed the SiC-C FGC layer to oxidize.

Functionally Gradient Materials, CVD, Levitaion, Carbon/carbon Composite, Oxidation Resistant, SiC, Coating 46

Unclassified Unclassified Unclassified

Summary

SiC-C functionally gradient coatings, (FGC), have been successfully deposited using a vertical cold wall chemical vapor deposition (CVD) reactor of our own design and construction. These coatings were deposited on graphite substrates and range in thickness from 400 μm to 6 mm. It should be noted that according to the literature, coatings deposited under the conditions used should grow at a rate of 1 mm per hour. The deposition rates for the coatings we have obtained are up to 6 times greater than those reported in the literature.(Wang et al., 1990) X-ray and auger analysis of the deposited coatings reveals that the composition of the coatings varies from graphite at the substrate/coating interface, to silicon carbide at the surface. The analysis also showed that the composition profile of the coatings mimics the composition profile of the reaction gases. High temperature thermal cycling between 25°C and 2000°C in argon, and rapid heating to temperatures greater than 2100°C in an oxidizing atmosphere have shown that the FGC remains adherent to the graphite substrate and that it does not spall or crack.

To facilitate the coating of the entire surface of a substrate during a single CVD run, a new technique was developed which employs a electromagnetic fields to simultaneously levitate and heat a sample. This process produces a continuous coating free from the discontinuities found in coatings where multiple runs were required to encapsulate the entire substrate. At present, a patent is being sought for this new coating technique, Levitation Chemical Vapor Deposition (LCVD).

Thin IrAl intermetallic surface coatings, 5 to 10 μm thick, have been successfully deposited on polished SiC and the SiC-C FGC. The coatings were produced by alternately depositing layers of iridium (Ir) and aluminum (Al), then heating the coating to 700°C in vacuum. The resulting coating was observed to crack on both the polished SiC and the SiC-C FGC. X-ray analysis of the as reacted coating showed that all of the aluminum had indeed reacted with iridium to form IrAl. In addition, the X-ray analysis indicated that $IrSi_3$ had formed at the Ir - SiC interface. Upon exposure of the IrAl coated SiC - FGC to a high temperature oxidizing environment the surface was shown to form alumina (Al_2O_3).

Table of Content

List of Tables

List of Figures

1.0 Background

Over the past decade, a number of ceramic and metal "fine-composites" or more recently "nano-composites" systems, have been investigated for the purpose of obtaining improved fracture toughness and strength. Examples include TiC particles in SiC (Wei and Becher 1984), TiB_2 particles in SiC matrix (Taya et al., 1990), and SiC particulate in 6061Al matrix (Taya et al., 1991a). The second phase is primarily used to enhance the fracture toughness of ceramics via a variety of toughening mechanisms, and to increase the yield stress and the modulus of elasticity of metal. In general, optimum properties of these composites are obtained when the second phase is *uniformly* distributed throughout the matrix. However, unique and new properties may arise if the second phase is purposely distributed *inhomogeneously* (Taya et al., 1991b, Hirai and Sasaki, 1991; Sasaki and Hirai, 1991; Sasaki et al., 1990). These materials with such inhomogeneous microstructure were first termed "Functionally Gradient Materials (FGM)" by a small research group at Tohoku University, Japan. Subsequently, the Japanese government (under MITI) sponsored a large R&D effort by forming a cohesive team consisting of industries, government research laboratories and universities over the period 1987-1991, of which results have recently been summarized and published as a monograph (Watanabe, 1993). Taya was involved in part of the FGM project while he was on leave at Tohoku University during the 1989-1991 period, mainly working with Professor Watanabe in modeling several structure-property relations (Muramatsu et al., 1990; Taya et al., 1991b). Despite early efforts by Japanese researchers, there exist a number of technical problems to be solved and new directions to be explored, to which the present proposal is addressed.

Compositionally and/or structurally graded materials have been used frequently in optics and electronics. For example, graded-index optical fibers are designed and used to reduce model dispersion of optical signals (Gambling et al., 1979). Graded-layer epitaxy is another example of the successful accommodation of lattice mismatches between the substrate and an epitaxial thin film. However, the application of FGMs to high temperature structural coatings is rather new. Figure 1 demonstrates requirement map of high temperature materials in various aerospace applications. Domain A denotes the requirement for thermally insulating materials such as skin material for National Aero-Space Plane (NASP) where no cooling and low thermal conductivity are required for short time use. Domain B represents the material for jet engine and gas turbine components where air cooling is predominant and the material must be durable for many hours (up to 20 hours for jet engines and 10^4 hours for turbine engines). The materials in Domain C are primarily for use in short time-but thermally conductive with rocket engine material as an example. Arrow markers in Figure 1 denote the anticipated improvement accompanying the use of FGM systems. Whatever the applications may be, ceramic-metal bonded structure has been widely used. For example, ceramic blades are mechanically attached to a metal rotor through slots to avoid the fracture due to high thermal stress induced by the mismatch of the coefficient of thermal expansion (CTE) between the ceramics and metal. This mechanical joining is known to cause fretting fatigue under certain loadings. The concept of FGM is an alternate method to diffuse the otherwise high thermal stress field at work around the ceramic-metal interface. Figure 2

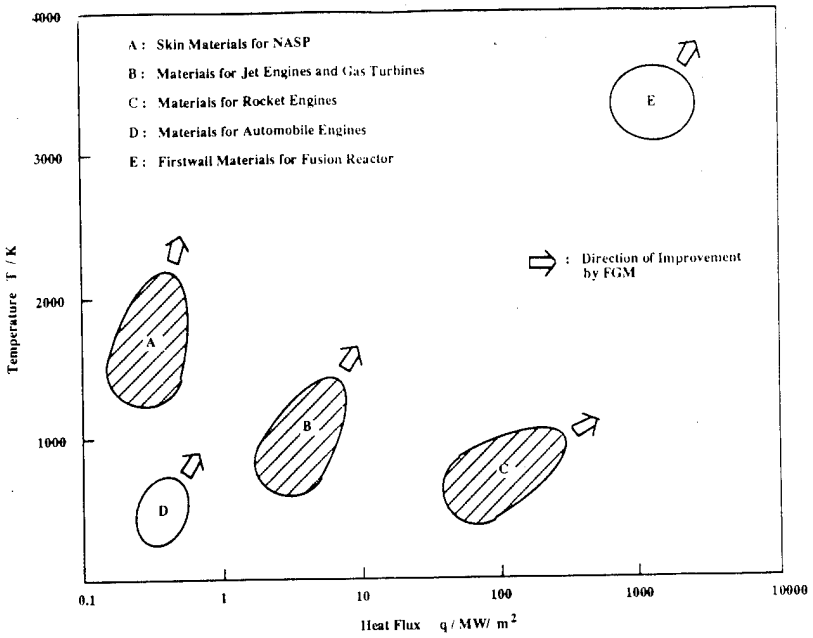

Figure 1 Requirement map for high temperature materials in various applications.

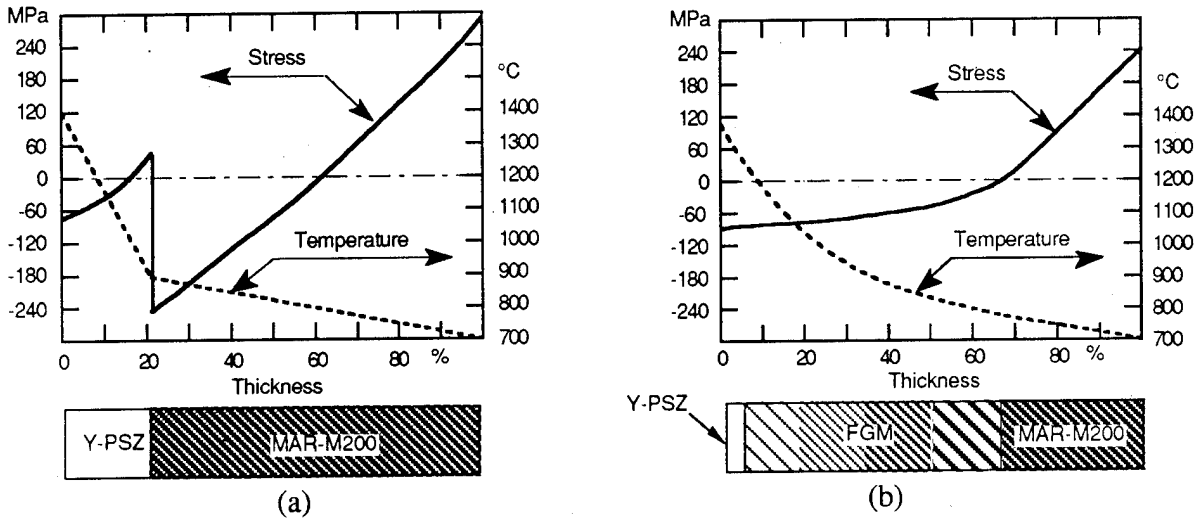

Figure 2 Distributions of one-dimensional stress and temperature within a metal (MAR-M200)/ceramic (Y-PSZ) bonded material with in-plane constraint: (a) without FGM interface, (b) with FGM interface (Watanabe, 1993).

illustrates the effectiveness of using FGM layer for reducing the stress field at the interface of ceramic (Y-PSZ) and metal (MAR-200) when the ceramic-metal component subjected to large temperature differential and in-plane constraint (Watanabe, 1993).

For the practical applications of FGMs in these severe high temperature environments, however, a number of fundamental scientific issues must be properly addressed. These include; (i) the criteria for choosing FGM systems, (ii) processing of the FGM systems, and (iii) FGM stability under a variety of thermal, mechanical and environmental conditions. It is important to investigate how the stress induced by thermal mismatch is accommodated in a FGM system and its effects on the thermo-mechanical behavior of the FGM system. The relationship between the graded structure, material stability and mechanical properties is not predictable *a-priori* and is a new area for investigation.

The term FGM used in the present proposal refers to "Functionally (or more precisely compositionally) Graded Materials" (FGMs). FGMs can be categorized as two types: Functionally Graded Coatings (FGCs) and Functionally Graded Interfaces (FGIs). In the former systems, a coating (material A) is bonded to a substrate (material B) where the thickness of the material A is considerably smaller than that of the material B, whereas the thickness of materials A and B are of the same order of magnitude in the latter systems.

The FGM concept relies on an inhomogeneous dispersion to purposely tailor the material characteristics from one side to the other. This proposed research will investigate metal matrix composite (MMC) graded coatings. One primary goal for the MMC coating will be to reduce the residual stresses induced by thermal expansion mismatch. Thus, the proposed research is aimed at studying the relaxation mechanisms for the ceramic-metal bonding with FGM microstructure both at macro-level (elastic/plastic/creep analysis) and at micro-level (dislocation punching).

2.0 Development of Stationary CVD for the Synthesis of FGC

2.1 The CVD Apparatus; Description and Development

The CVD unit is a low pressure, cold wall, vertical reactor, 2 feet tall and 1 foot in diameter. It is constructed of stainless steel and coated with water cooled copper tubing to maintain a constant chamber wall temperature during operation, see Figure 3. Sample heated is provided by a 15 kW induction heater operating at 315 kHz. The chamber is capable of being evacuated to 10^{-6} torr and back filled with purified argon. This ensures a contamination free environment in which to deposit the coating. All reactant gases are purified prior to introduction into the chamber via desiccators and oxygen scrubbers. The rates at which these gases are introduced are controlled by mass flow controllers. Liquid sources of reactants can be placed into a constant temperature bath and delivered to

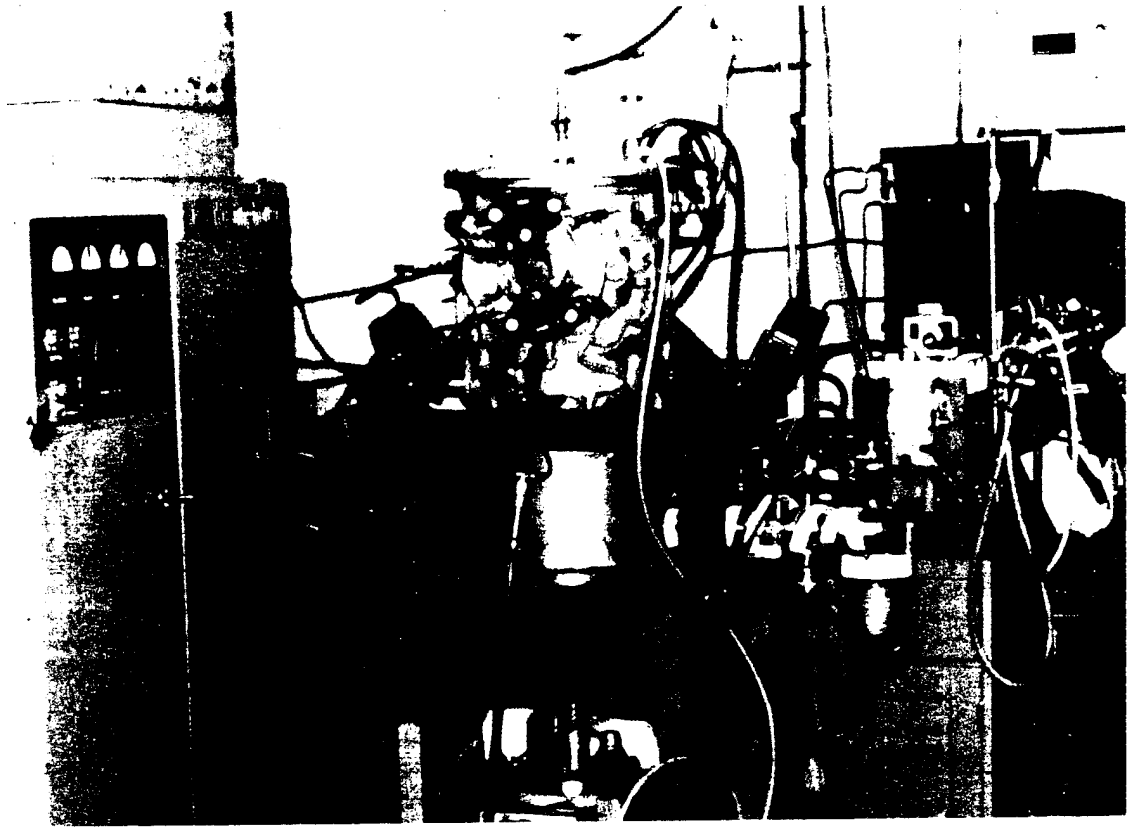

Figure 3. Photograph of CVD reactor and power supply.

the chamber via a carrier gas. Waste gases generated during deposition are scrubbed in a sodium hydroxide scrubber, followed by two liquid nitrogen cold traps. A schematic of the CVD unit is shown in Figure 4.

Operational difficulties for this reactor had to be overcome in two areas. First, the gas inlet for the chamber and the sample were too far apart. This created a poor quality coating due to re-incorporation of waste products into the reactant gas stream. Since the sample position and the gas inlet position were fixed by the geometry of the chamber, a means of delivering the reactant gas in a controlled manner to the sample had to be devised. Therefore, a quartz shroud was fabricated to surround the sample and control the gas flow within the chamber. Second, the operation of the induction coil within the low pressure CVD unit caused arcing and a glow discharge. These discharges were detrimental in two ways, first was to rob power from the coil thus reducing the temperature of the substrate and second, to melt small holes through the chamber wall creating the possibility of explosion. To combat the this problem a high power feed through was obtained that put the chamber walls at the same ground potential as the power return line. Additionally, the operating parameters for coating were modified to allow for operation at pressures where arcing is less likely.

2.2 Experimental Procedure

The gases used to synthesize the SiC-C FGC are propane (C_3H_8), hydrogen (H_2), and silicon tetrachloride ($SiCl_4$). The overall deposition reaction is based on the following chemical equation:

$$\mathbf{SiCl_4(g) + C_3H_8(g) + H_2(g) => SiC(s) + 2\ C(s) + 4\ HCl\ (g) + H_2(g)}$$

In order to achieve the compositional gradient in the coating, the Si to C ratio is increased from 0 to 2.0 during the deposition run, see Figure 5. By altering the rate of change of the Si to C ratio any profile can be achieved. For example, the profile can be linear, exponential, logarithmic, or any combination of these. The flow rates for these experiments are:

Flow rates (10^{-6} m^3/sec)	C_3H_8	0.58
	H_2 ($SiCl_4$)	0.67 to 11.2
	$SiCl_4$	0.21 to 3.47
	H_2 (extra)	8.34

Depositions runs were performed at 1400°C, at a pressure of 100 torr, for 71 minutes.

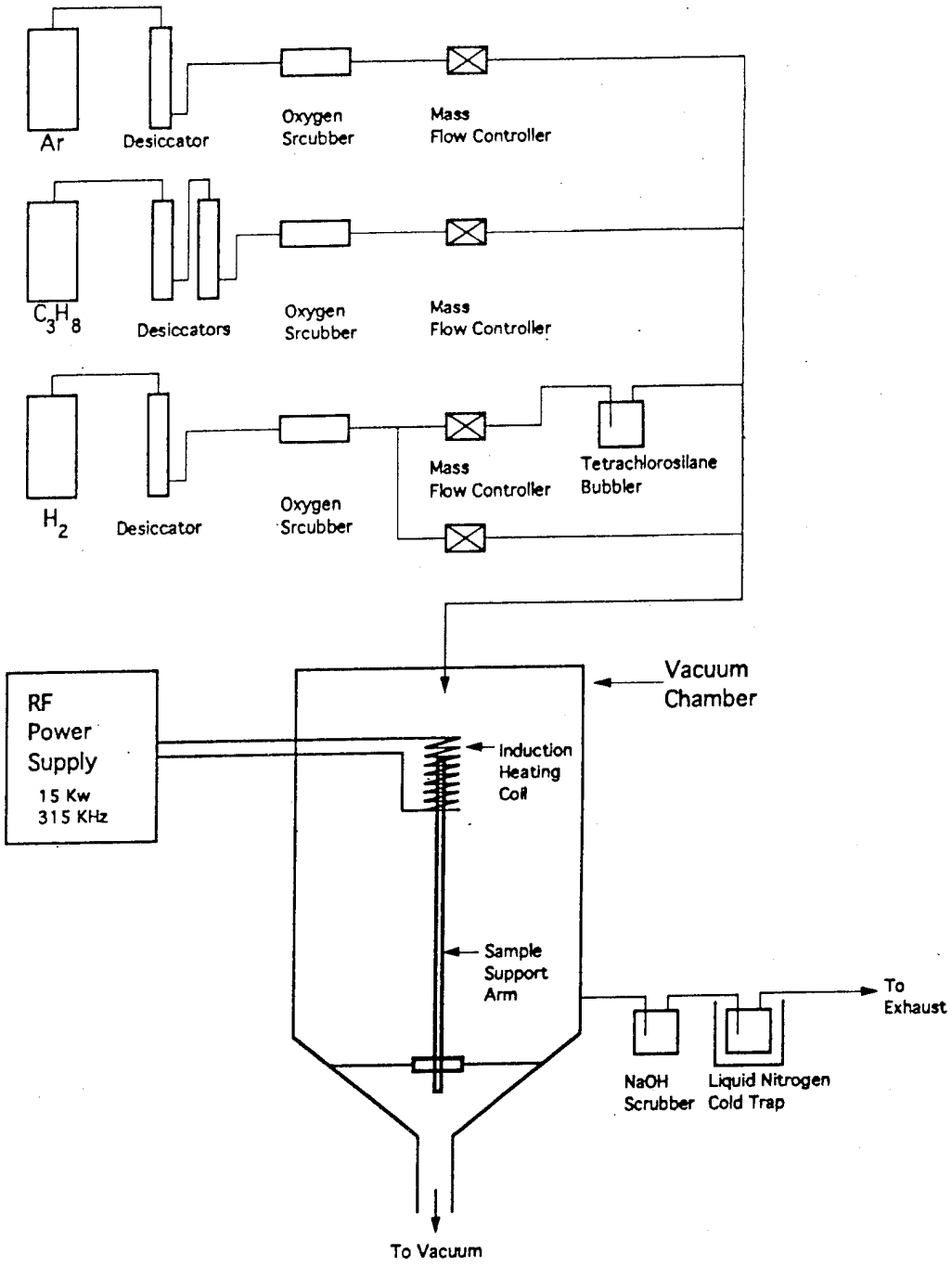

Figure 4. Schematic of CVD reactor and input gas control system.

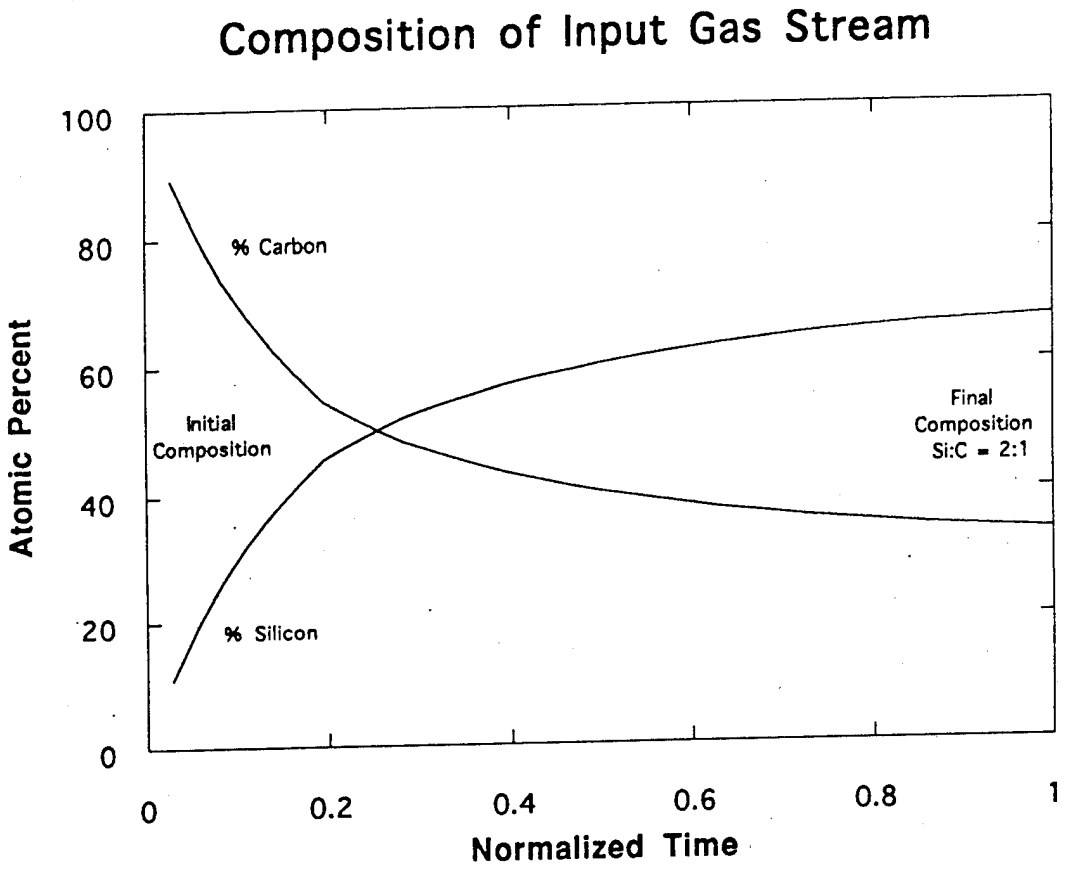

Figure 5. Graph of Si to C ratio in the reaction gas stream.

2.3 Characterization of Materials

At present, two different coating morphologies have been deposited and examined using both optical microscopy and scanning electron microscopy (SEM). The first coating is approximately 400 μm thick, dense and strongly bonded to the substrate, see Figure 6. The other is 6 mm thick, dense at the surface yet contains a weak porous region, see Figure 7. Both coatings were deposited under the same parameters and posses the same compositional profile. The only variation between the two was distance from the substrate to the reactant gas inlet. In the case of the 400 μm thick coating, the reaction gas inlet to substrate distance was large, approximately 3.5 inches. While in the case of the 6 mm thick coating the distance was approximately 1.0 inch.

X-ray analysis of both morphologies indicates that the coating changes from graphite plus silicon carbide at the substrate/coating interface to pure silicon carbide at the surface, see Figure 8. Auger analysis of the coatings indicate a changing silicon to carbon ratio through the coatings thickness, see Figure 9. The compositional profile derived from the auger analysis, Figure 10, shows how the percentages of silicon and carbon changes from almost no silicon at the substrate/coating interface to 50% silicon, 50% (carbon i.e. 100% SiC) at the surface. Also included in Figure 10 is the expected compositional profile of the coating derived from the reaction kinetics. Excellent agreement between the expected composition and the actual composition of the coating was achieved, except when a mechanical problem caused a spike in the silicon content of the reaction gas stream. However, this spike in the silicon content of the coating indicates the degree of control of the coating's composition.

A hardness profile of the functionally gradient coating indicated that the hardness increased from 158 VHN at the graphite/coating interface to between 3500 to 4200 VHN in the pure SiC at the surface, see Figure 11.

2.4 Thermo-Stability Test and Characterization

Preliminary high temperature stability tests have been performed on samples coated with the 400 μm thick coating. Two samples were thermally cycled in argon between 25°C and 2000°C for 10 and 30 cycles. In both tests the coating showed no signs of cracking or spalling, the coatings remained strongly adhered to the graphite substrate. Two other samples were flame tested in air for one and five minutes. For this test, each sample was directly exposed to the flame of a hydrogen-oxygen

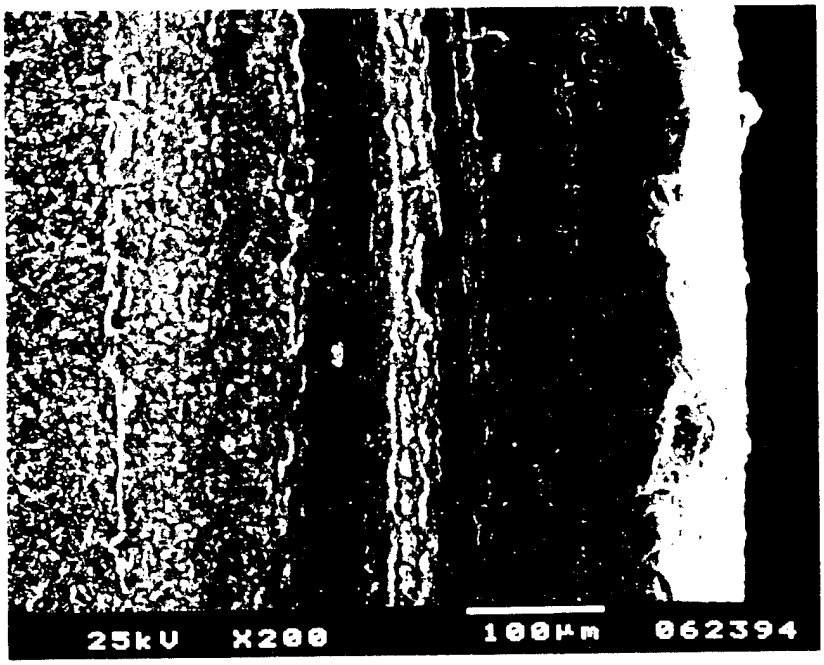

Figure 6. SEM micrograph of the 400 µm thick coating.

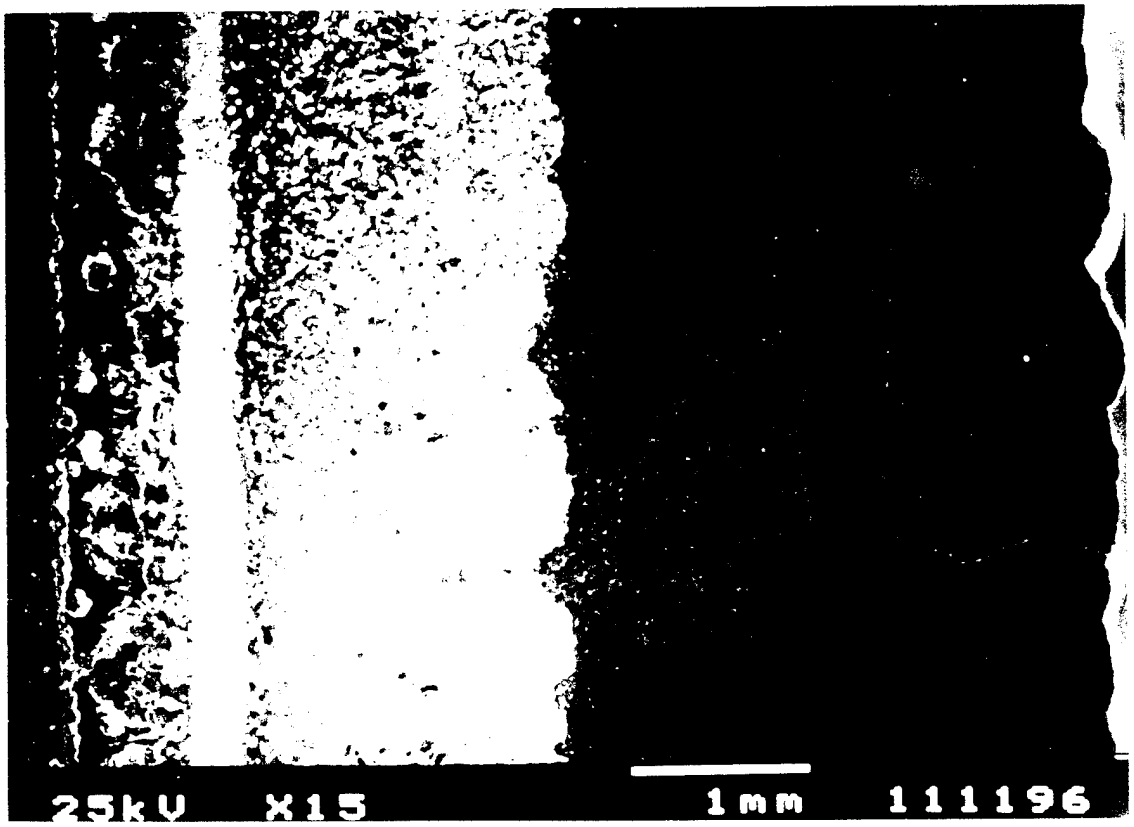

Figure 7. SEM micrograph of the 6 mm thick coating.

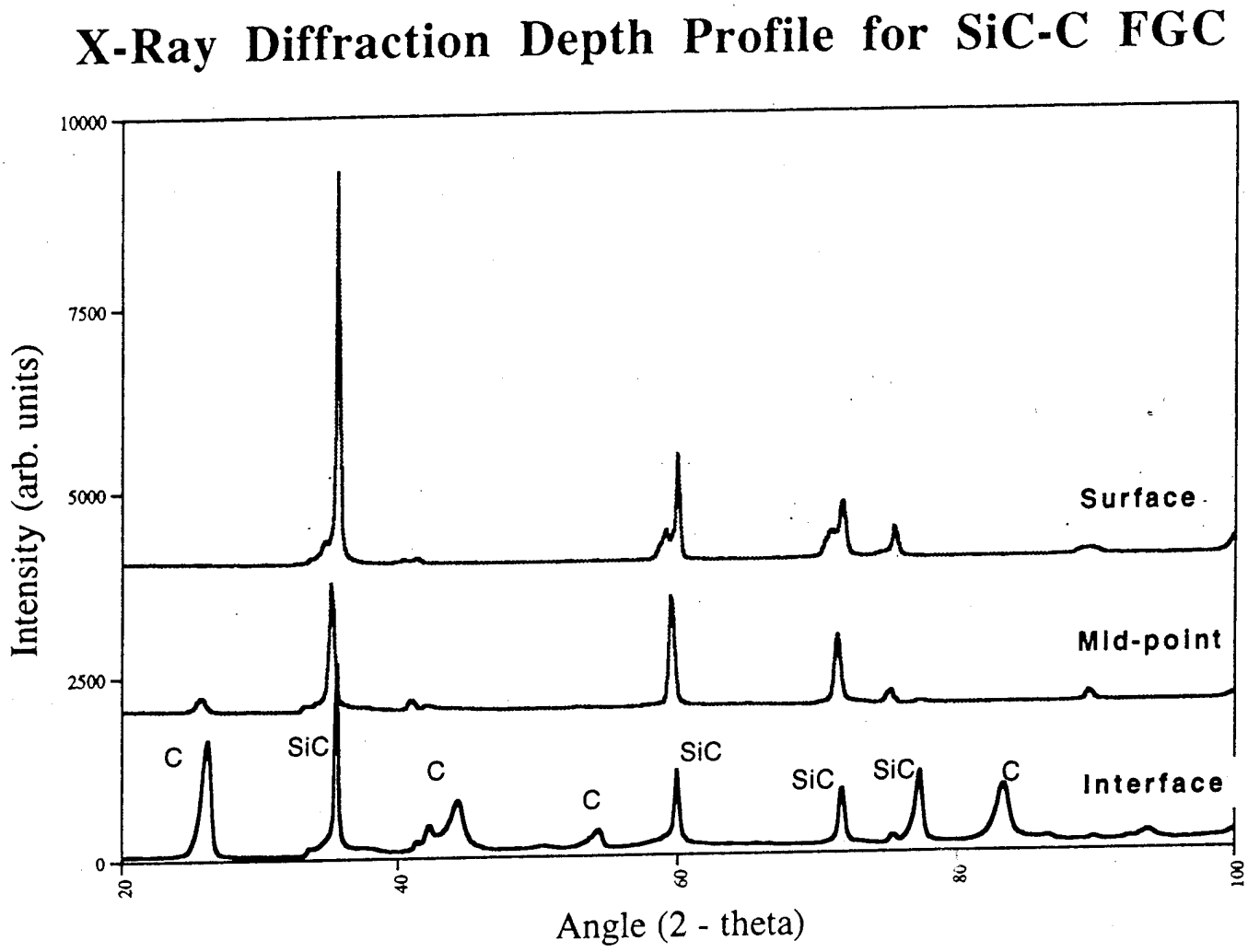

Figure 8. X-ray analysis showing SiC plus C at the substrate/coating interface and pure SiC at the surface.

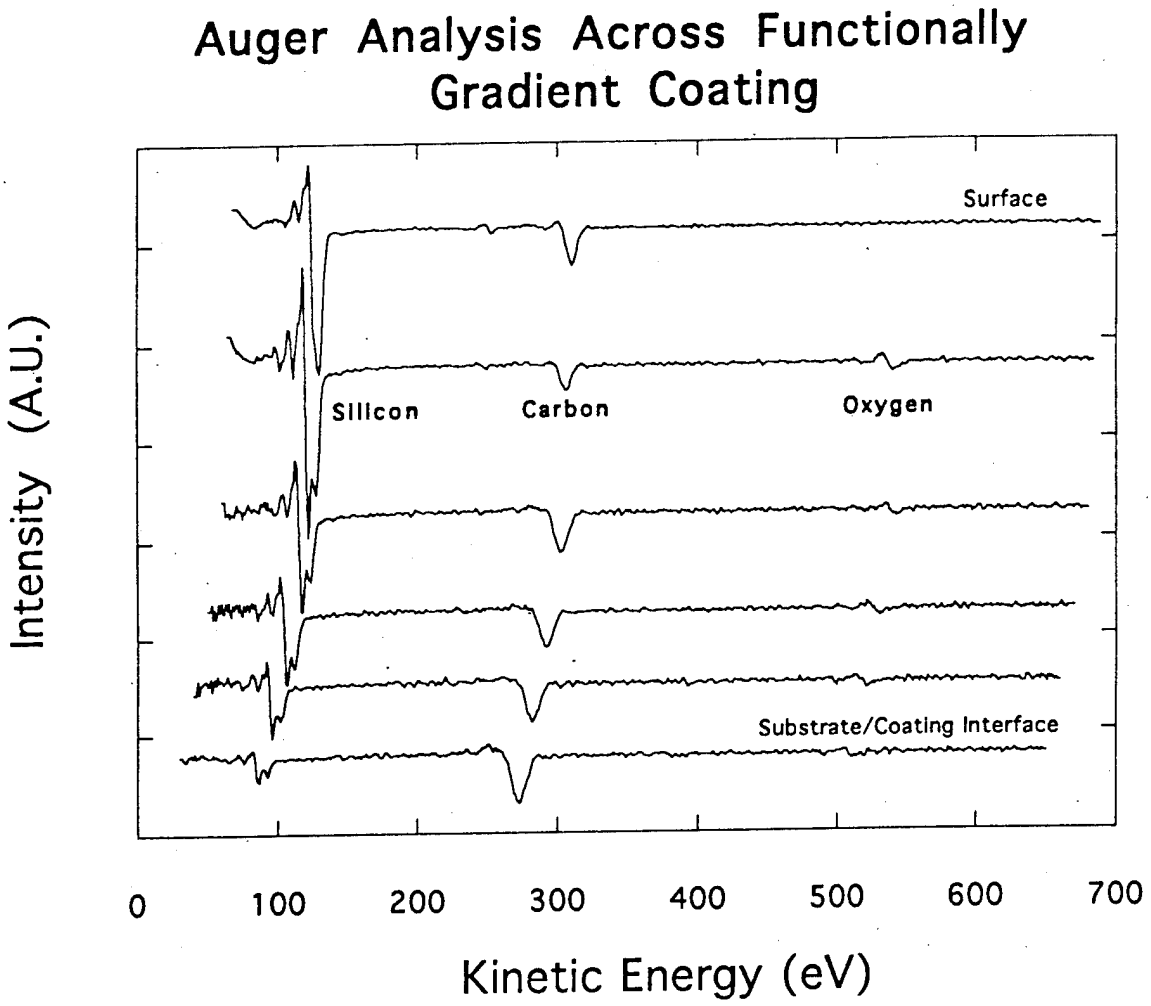

Figure 9. Auger analysis across the functionally gradient coating.

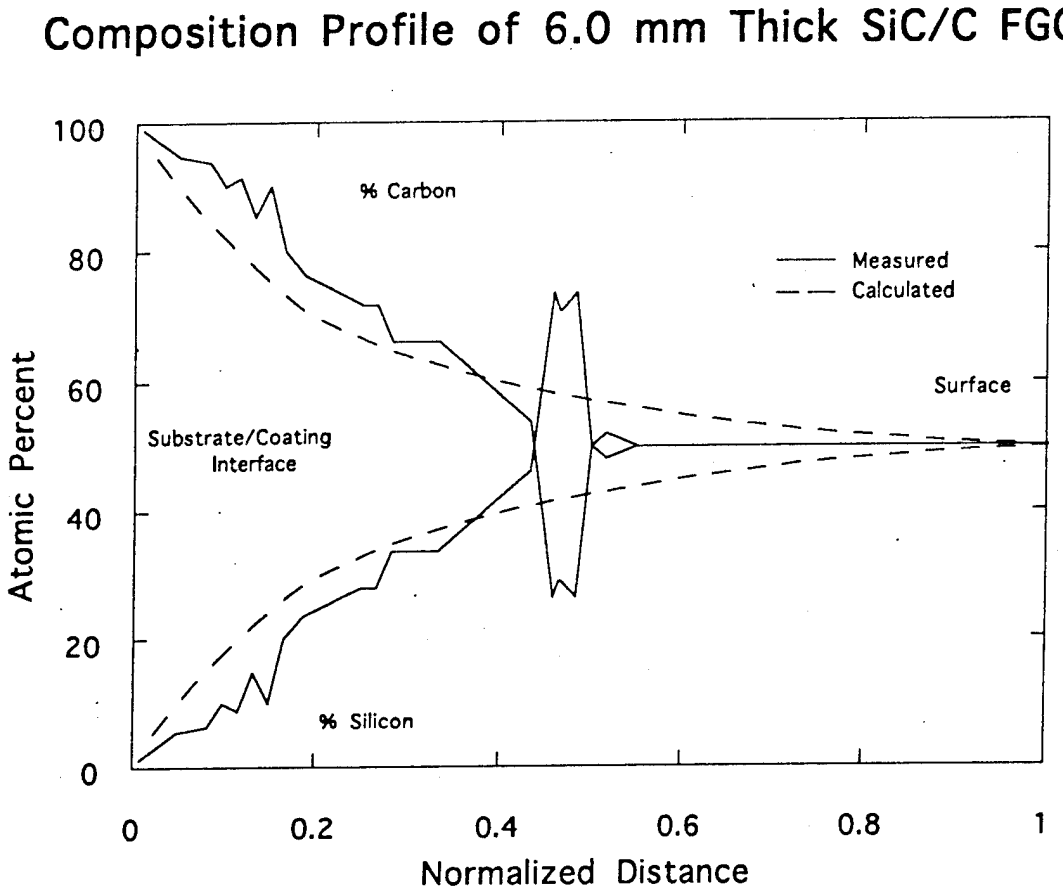

Figure 10. Calculated and actual compositional profile across FGC.

torch set to burn oxygen rich. The flame from this torch was in excess of 2100°C. In both instances the coating remain adhered to the substrate, there was no evidence of spalling. The surface of the sample which was exposed to the flame for five minutes showed signs of the formation of a glassy phase on the surface. The glassy phase was silica an expected by-product from the exposure of silicon carbide to a high temperature oxidizing environment. One disturbing result from the flame test was the high degree of erosion of the graphite substrate from the uncoated surfaces, see Figure 12.

3.0 Development of Levitation CVD (LCVD) for the Synthesis of FGC

Conventional CVD operations require some type of mechanical support of the substrate. The presence of the support created discontinuities in the coating. Therefore, to coat the entire surface of a part requires a minimum of two coating runs. When functionally gradient coatings are being deposited these problems are compounded. Due to the nature of FGC a second coating operation to cover the discontinuities in the first only introduces more discontinuities. What is needed is a CVD process which allows a substrate to be freely suspended within the gas stream. To meet these requirements a new CVD process was developed which employs electromagnetic fields to simultaneously levitate and heat the substrate.

3.1 Concept of LCVD

The concept of using electromagnetic fields to levitate a conductive sample was first proposed by Muck in 1923 (Muck, 1923). Muck theorized that when a conductive material was placed into an induction coil the magnetic field generated by the coil would produce eddy currents within the sample. The eddy currents within the sample would generate their own magnetic field. Since this field opposes the field generated by the coil the two magnetic fields should repel and the sample will levitate. Once the sample has been levitated it can be coated on all sides during a single coating operation, thereby eliminating coating discontinuities caused by the sample support mechanism.

3.2 Adaptation of CVD Unit to LCVD

Adaptation of the existing CVD unit to allow for levitation of the substrate was extremely simple, only two changes were required. First, a different coil design was needed and second, a retractable support rod which could be lowered when the substrate levitates was fabricated. The initial design of the CVD unit called for a cylindrical induction coil for heating, see Figure 13. By replacing this coil with a conical induction coil, Figure 14, the substrate could be levitated during deposition. The

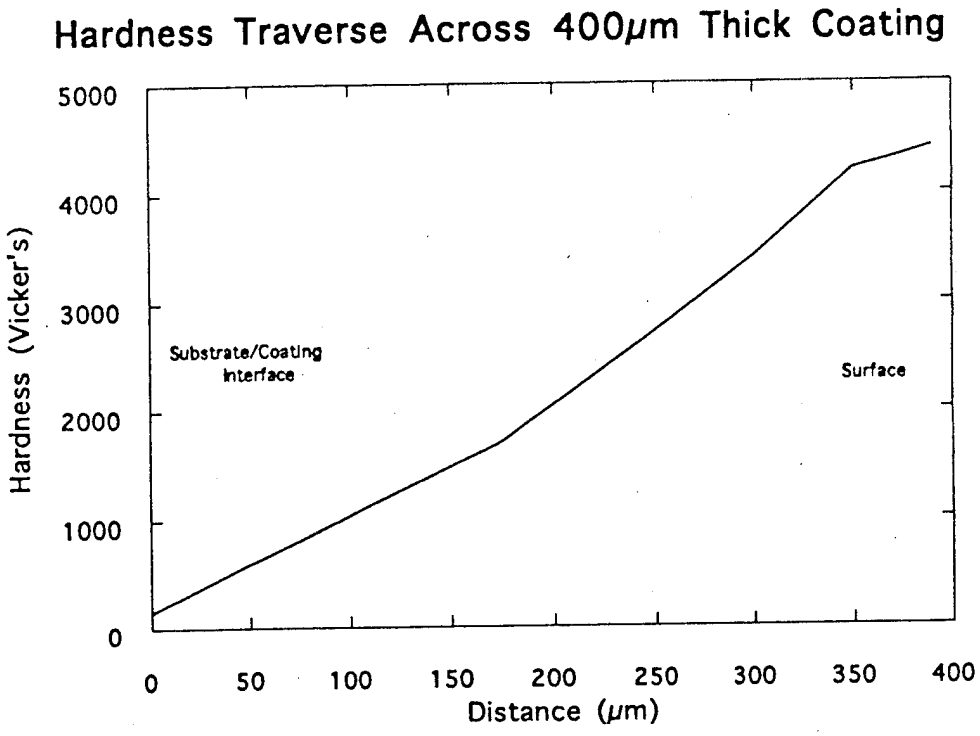

Figure 11. Microhardness traverse across 400μm FGC.

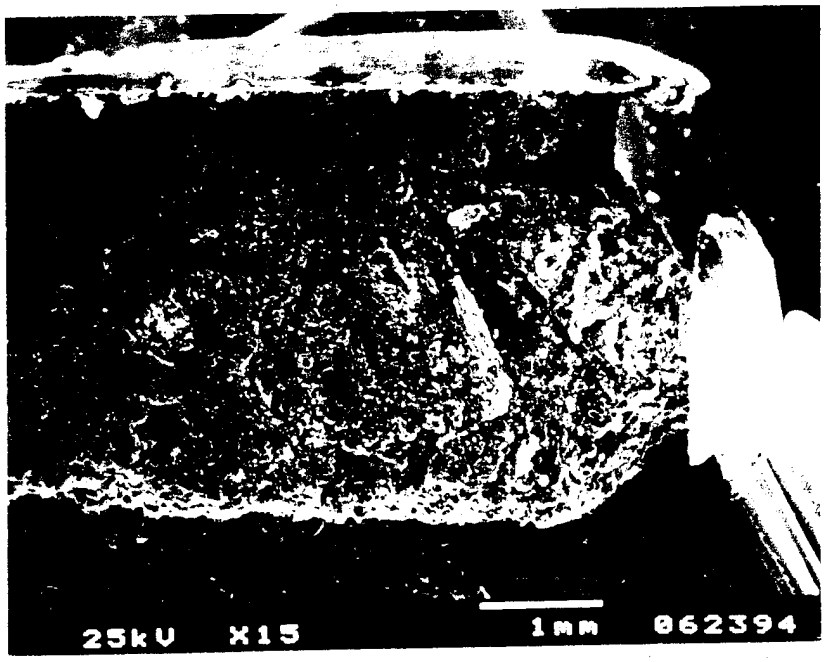

Figure 12. SEM Micrograph of sample exposed to oxygen rich hydrogen flame for 5 minutes.

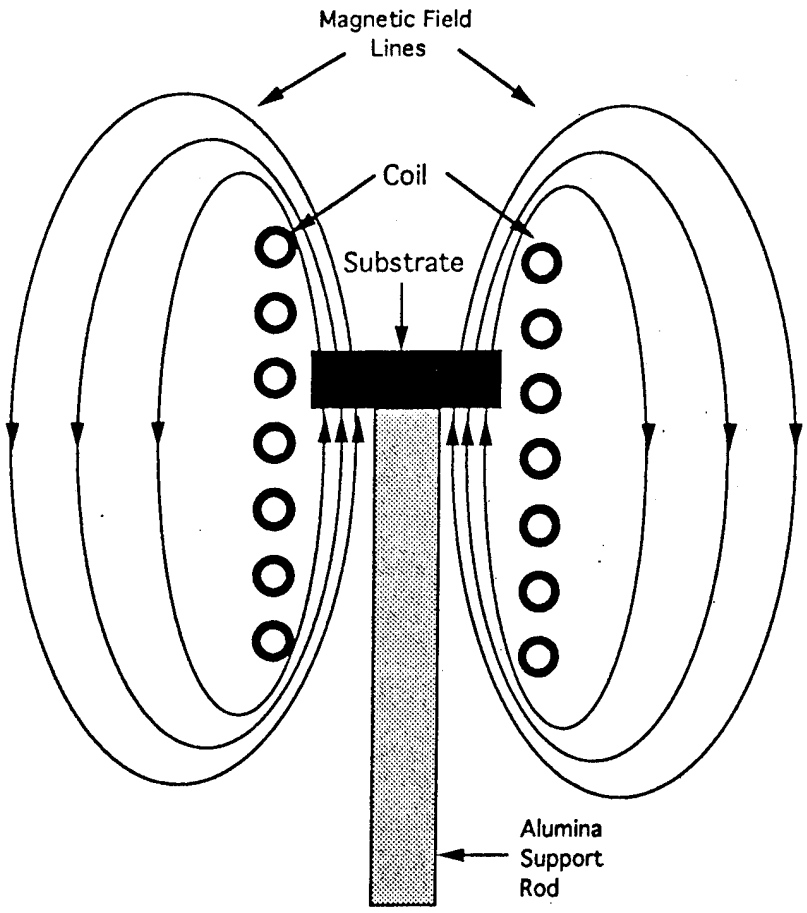

Figure 13. Schematic of conventional induction coil

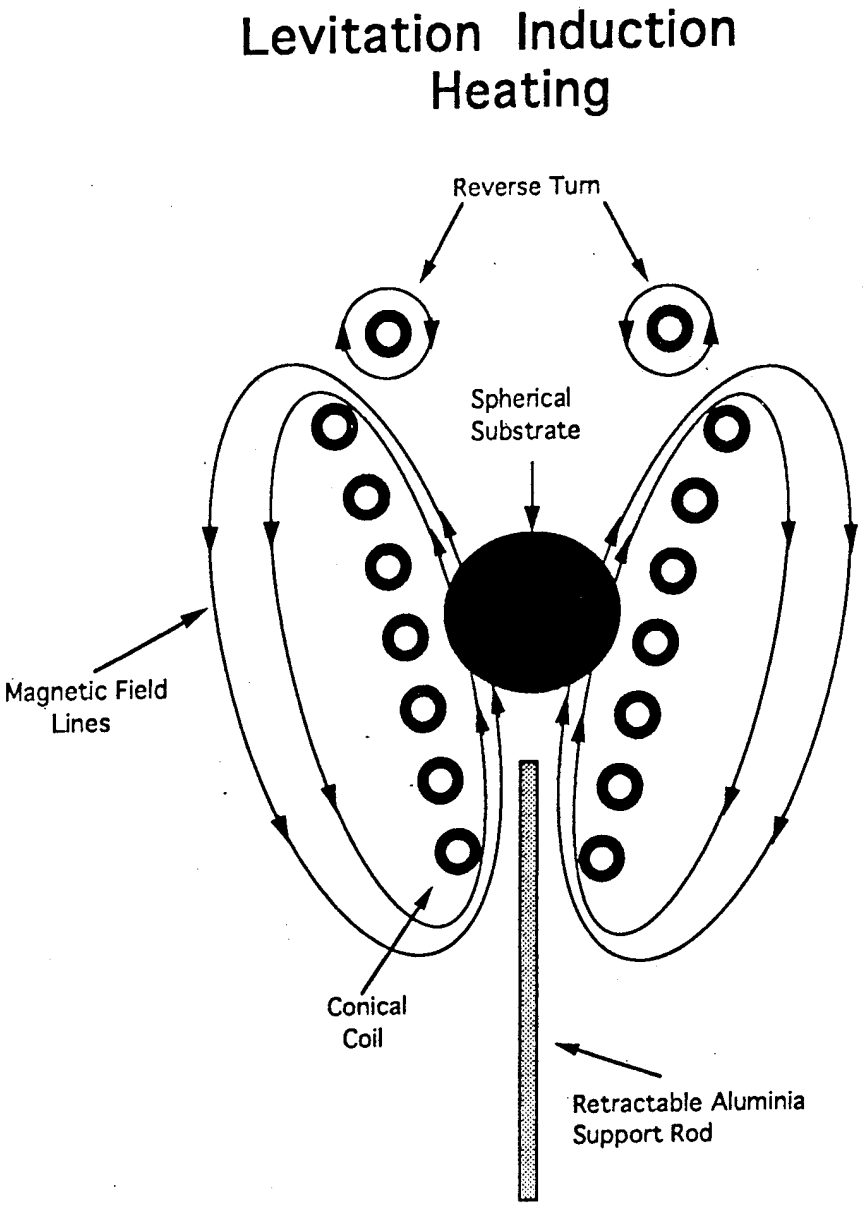

Figure 14. Schematic of levitation induction coil.

new coil was constructed from 0.125 inch copper tubing, contains five turns plus one reverse turn, it has a 25 degree included angle, and the bottom coil diameter in 1.5 cm. An alumina support rod was installed which could be manipulated from outside the chamber. This was required so the substrate could be maintained within the coil until the magnetic field could be established. Once the substrate was levitated the support arm could be lowered so as not to interfere with the gas flow.

3.3 Experimental Procedure

The experimental procedure for the fabrication of coatings using LCVD is the same as for conventional CVD. Presently, the only difference between the two techniques is the shape of the substrate.

A schematic of the LCVD reactor is shown in Figure 15. As can be seen, the only changes to the conventional CVD reactor were the addition of the movable substrate support and changing the induction coil. Again, the RF power supply operates at 15 kW and 315 kHz. The precursor gases are $SiCl_4$ and C_3H_8, with H_2 used as a carrier gas for the $SiCl_4$. Reactant gases enter at the top of the chamber and are directed over the substrate via a quartz shroud. An alumina rod holds the substrate away from the coil until it begins to levitate. The rod is retracted before the deposition begins so as not to interfere with the gas flow. After the deposition, the alumina rod can be inserted to support the substrate as it cools.

In order to characterize the new technique, the LCVD reactor was first used to deposit silicon carbide films under various conditions. Three different chamber pressures were combined with three flow rates to produce a series of nine samples, see Table 1. The SiC was deposited onto 1.9 cm diameter graphite spheres weighing approximately 6.5 g. The substrate material was SiC-12 supplied by Toyo Tanso USA Inc. A deposition time of 15 minutes was used for each sample at a temperature of approximately 1700°C, as determined by optical pyrometry.

Table 1 Flow rates and chamber pressures for LCVD of SiC.

	Flow Rates (cc/sec)		
Chamber Pressure (Torr)	$H_2(SiCl_4)$ 11.17 C_3H_8 0.58	$H_2(SiCl_4)$ 5.58 C_3H_8 0.29	$H_2(SiCl_4)$ 2.79 C_3H_8 0.145
250	X	X	X
350	X	X	X
500	X	X	X

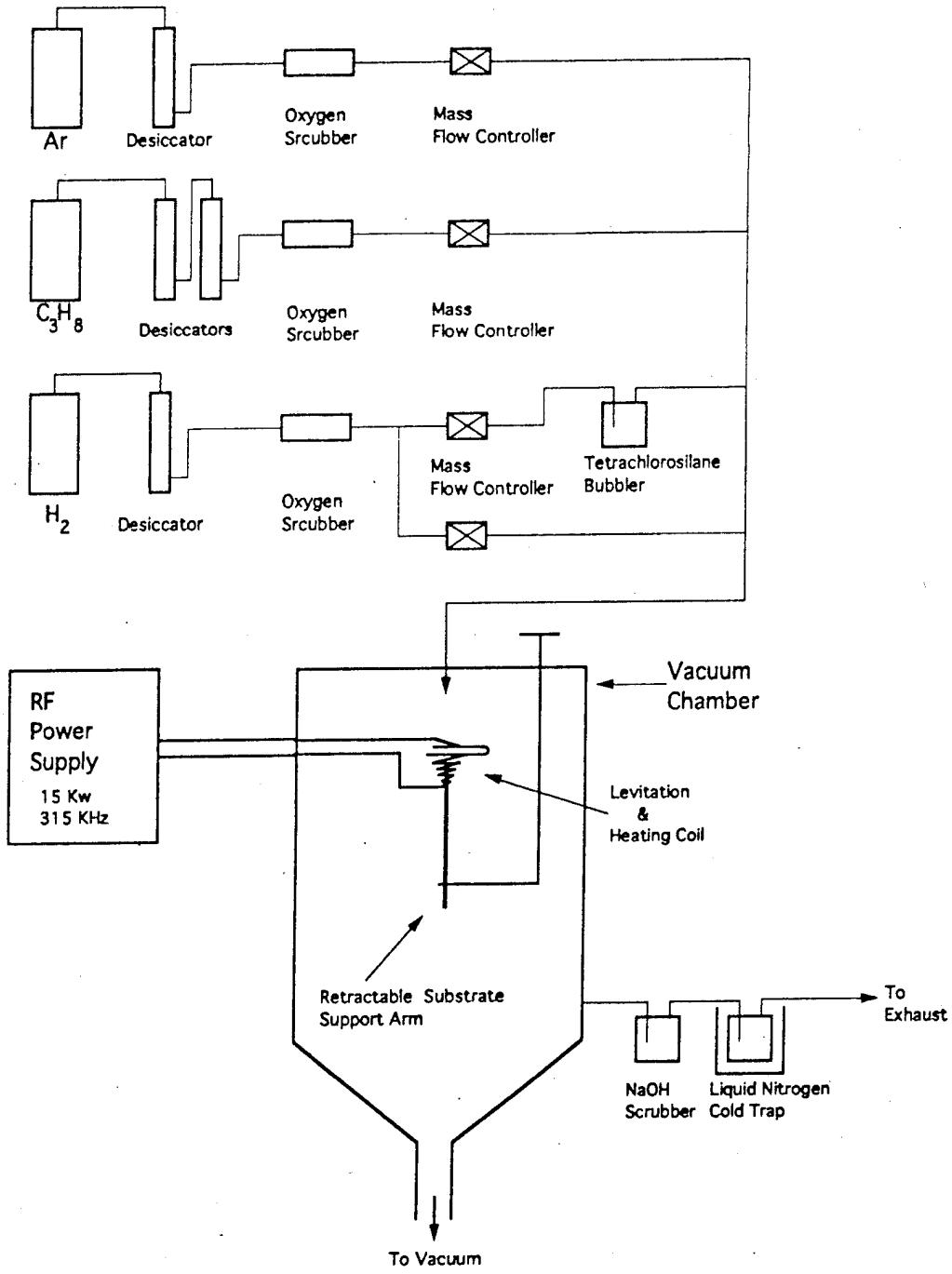

Figure 15. Schematic of LCVD reactor and input gas control system.

3.4 Characterization of Coating

X-ray diffraction (XRD) was used to characterize the SiC coating. Figure 16 is a XRD pattern representative of all samples produced. This pattern shows β-SiC which is consistent with SiC produced at temperatures greater than 1500°C (Choi et al, 1991; Parretta et al., 1991; Wang, et al., 1991).

The micrographs in Figure 17 show the cross sectional thicknesses of the nine samples. All micrographs were taken at the same magnification for comparison purposes. It was found that the thickness of the coating at each flow rate was similar regardless of the chamber pressure. The average thickness at the $H_2(SiCl_4)$ = 2.79cc/sec rate was approximately 60μm, Figures 17 (a), (b), and (c).

The coatings produced with the flow rate of $H_2(SiCl_4)$ = 5.58cc/sec are shown in Figures 17 (d), (e), and (f). Although the variation in thickness was greater at this flow rate, the average thickness of the coatings was consistently greater than those produced using the lower rate. Disregarding the poor coating quality in Figure 17 (f) the average thickness is about 235μm for this flow rate.

At the high flow rate of $H_2(SiCl_4)$ = 11.17cc/sec, Figures 17 (g) through (i), the coatings were much thicker than those produced at previous flow rates with an average thickness of approximately 406μm. The line of porosity near the midpoint of the coatings in Figure 17 (h) and (i) was due to the abrupt flipping of the substrate in the coil about halfway through the deposition (7 to 8 minutes). Again, the deposition rate was not dependent on the chamber pressure, but rather on the flow rates of the reactant gases. The trend seen in Figure 17 clearly indicates that increasing the relative flow rate of the gases produced a greater deposition rate.

Several researchers have reported changes in surface morphology to be dependent on the temperature of the deposition (Choi et al, 1991, Parretta et al., 1990; Wang, et al., 1991). At a constant pressure and constant flow rate, increasing the deposition temperature produces a trend from a smooth columnar growth to a faceted growth (Choi et al, 1991, Parretta et al., 1990). Similar changes in morphology were produced in this research by varying the chamber pressure and holding the temperature and flow rate constant. The surface morphology of coatings produced at the high flow rate, $H_2(SiCl_4)$ = 11.17 cc/sec, are shown in Figure 18. The trend from a smooth deposition to a faceted growth was seen as the chamber pressure was decreased. The fine grained, smooth surface of the high pressure (500 torr) coating is shown in Figure 18 (a). As the chamber pressure was decreased to 350 torr the structure coarsened and became fine grained and nodular, see Figure 18 (b). The low chamber pressure (250 torr) produced an even larger nodular structure, Figure 18 (c), however it is somewhat more course and tends to be faceted. This

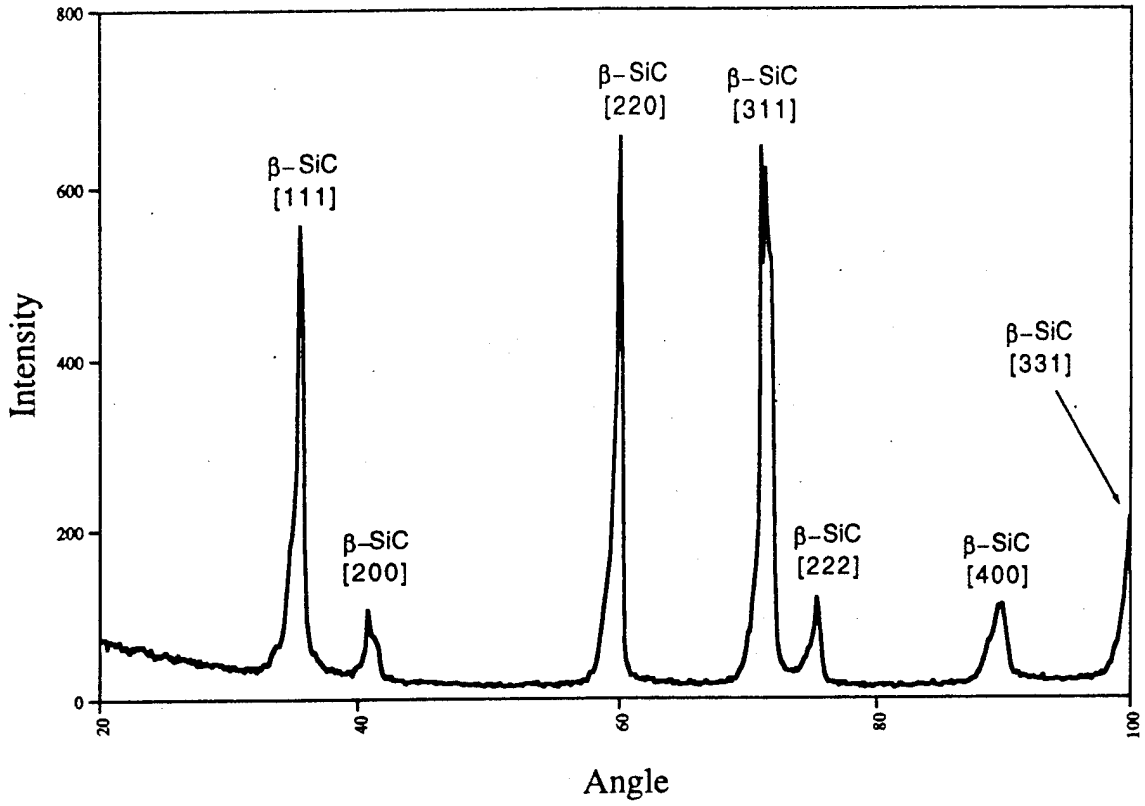

Figure 16. X-ray analysis of β-SiC deposited using LCVD.

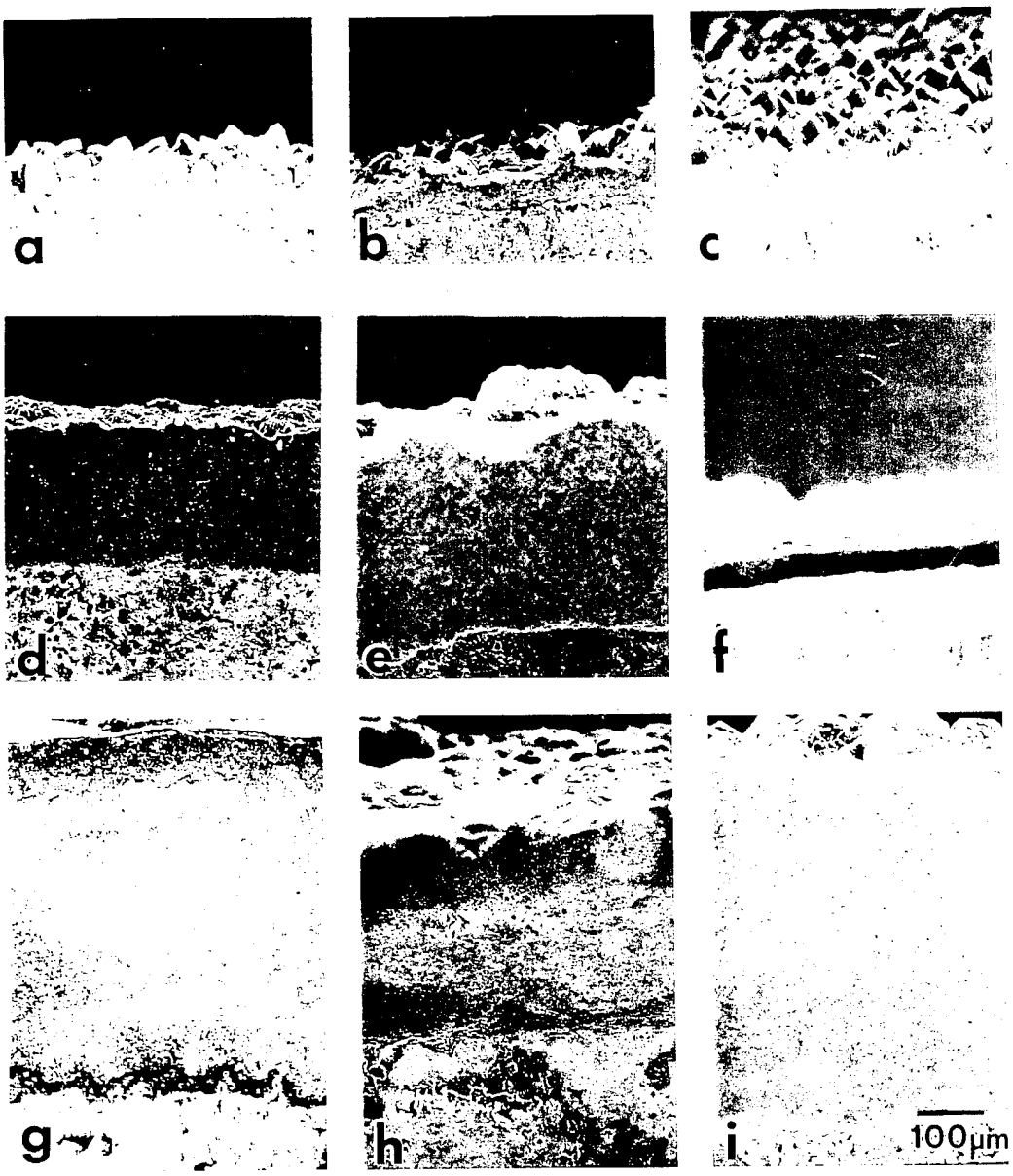

Figure 17. Coating thickness at various chamber pressures and flow rates.

	Chamber Pressure (Torr)		
Flow Rates (cc/sec)	500	350	250
$H_2(SiCl_4)$ 2.79	a	b	c
$H_2(SiCl_4)$ 5.58	d	e	f
$H_2(SiCl_4)$ 11.17	g	h	i

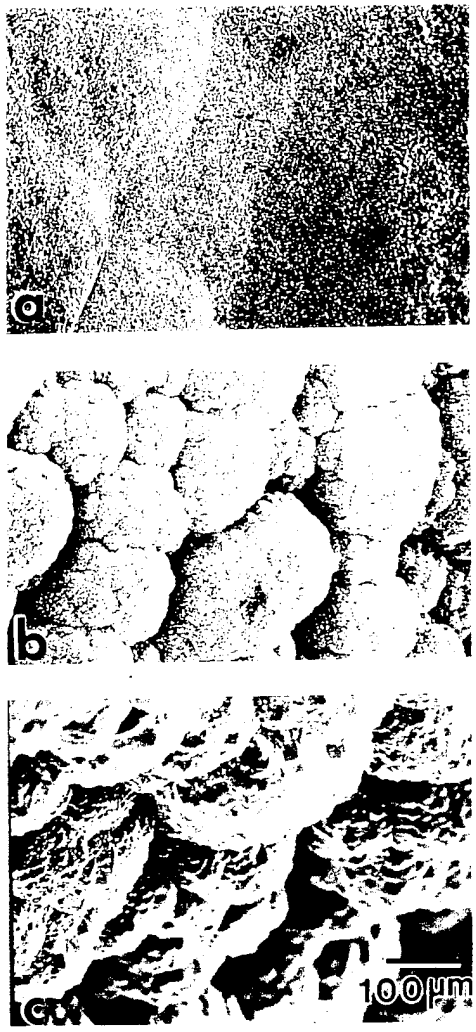

Figure 18. Surface morphology at a constant flow rate($H_2(SiCl_4$ = 11.17 cc/sec) and various chamber pressures.

shift in morphology was also observed by Parretti et al. (1991). However, in that work the precursor gas ratio was also varied and the shift was attributed to both the change in this ratio as well as the change in chamber pressure. In the present work, the precursor gas ratio was kept constant so the change in morphology can be attributed solely to the variation in the chamber pressure.

A similar trend in morphology was found when the flow rates were varied while the chamber pressures remained constant. The differences seen in Figure 19 show the trend from a smooth surface to an extremely faceted surface as the flow rate was decreased. Once again, the fine grained, smooth surface of the high pressure/ high flow rate coating is shown in Figure 19 (a). The structure becomes more nodular when the flow rate is decreased to $H_2(SiCl_4)$ = 5.58 cc/sec, Figure 19 (b). The low flow rate, $H_2(SiCl_4)$ = 2.79 cc/sec, produces an extremely faceted growth, Figure 19 (c).

Varying the flow rates and chamber pressures independently, allowed the effects of each parameter to be examined. Comparing Figures 18 and 19, the more drastic changes occurred when the flow rate was varied and the chamber pressure was held constant. Table 2 summarizes the changes in surface morphology at the various flow rates and chamber pressures. In general, there was a coarsening of the structure from the high chamber pressure to the low chamber pressure. Also, there was a trend towards a more faceted structure as the flow rate was reduced. These trends reflect the difference in growth mechanisms between the high and low flow rates and the high and low deposition pressures. At the high flow and high pressure conditions the reaction is limited by mass transport (diffusion) whereas at the lower pressures and lower flow rates the reaction is more controlled by surface kinetics (Pierson, 1992).

Table 2 Summary of the changes in morphology as a function of chamber pressure and flow rate for the LCVD system.

	Flow Rates (cc/sec)		
Chamber Pressure (Torr)	$H_2(SiCl_4)$ 11.17 C_3H_8 0.58	$H_2(SiCl_4)$ 5.58 C_3H_8 0.29	$H_2(SiCl_4)$ 2.79 C_3H_8 0.145
250	smooth	small nodular	faceted
350	fine grained w/ large nodules	med. nodular	faceted
500	large nodules w/ facets	small nodular w/ some facets	faceted

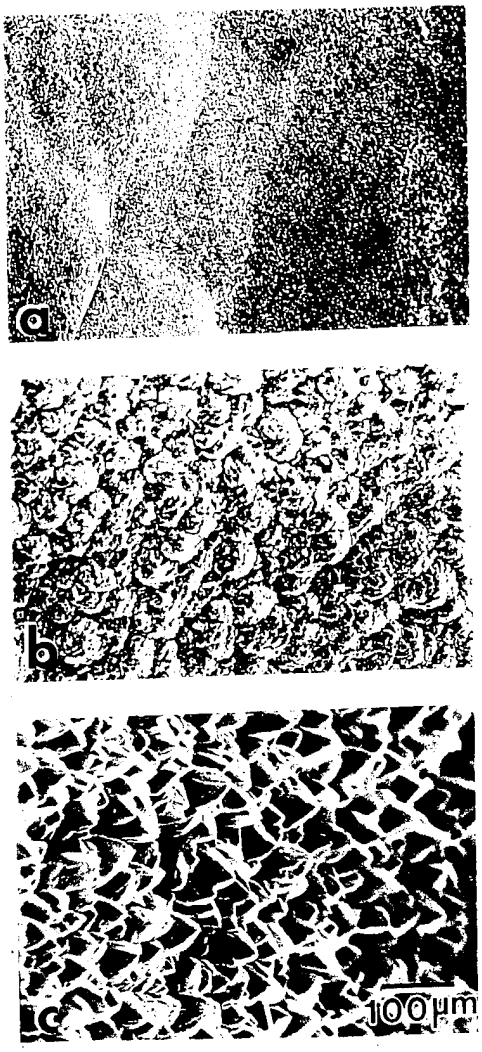

Figure 19. Surface morphology at a constant chamber pressure(500 Torr) and various flow rates.

4.0 Development of technique for the Deposition IrAl

The final stage of sample preparation involved the application of a coating of the intermetallic compound IrAl onto the SiC-C FGC. This was to examine the possibility of enhanced high temperature oxidation resistance. The intermetallic compound IrAl melts congruently at 2140°C and has been shown to form a protective oxide scale of Al_2O_3 at elevated temperatures. In addition, an Ir-rich layer forms below the oxide scale and acts as an oxygen diffusion barrier, providing additional oxidation protection for the bulk material (Clift et al., 1990).

4.1 Adaptation of Sputtering Unit

It was determined that the most cost efficient way to deposit a coating of IrAl on to the SiC-C FGC was by building up coating from alternating layers of pure Ir and Al. This procedure allowed for rapid deposition of the films using a combination of sputtering and evaporation. Therefore, the existing sputtering unit had to be adapted to enable the substrate to be transported from one deposition source to the other without having to break vacuum. To facilitate the transportation of the substrate a mechanical feedthrough was designed and built to provide the required motion. In addition, a hot stage capable of reaching temperatures of 900°C was designed, built, and placed on the end of the feedthrough to aid in the deposition of the Ir. Figure 20 shows a schematic of the sputter/evaporation chamber.

4.2 Experimental Procedure

In order to apply the IrAl coating, two thin film deposition techniques were used, sputtering and evaporation. The use of these two different coating techniques allowed us to take advantage of the rapid deposition rate of Al using evaporation, see Table 3 for the deposition parameters and rates. The thickness of each layer was varied so as to ensure the proper atomic ratio of Ir to Al, however, no individual layer was thicker than 6 μm. By alternating layers of Ir and Al, which were deposited by sputtering and evaporation respectively, a thick film can be built up. Subsequent heat treatment of this film in argon or vacuum to 700°C allows for the formation of the intermetallic compound IrAl.

Three different coating schemes on two different substrates were used for this experiment. The substrates were both CVD SiC, however, the first was monolithic SiC polished with 1.0μm diamond and the second was the SiC surface of the as deposited SiC-C FGC. The three different coating schemes are listed in Table 4.

Schematic of Sputtering and Evaporation System

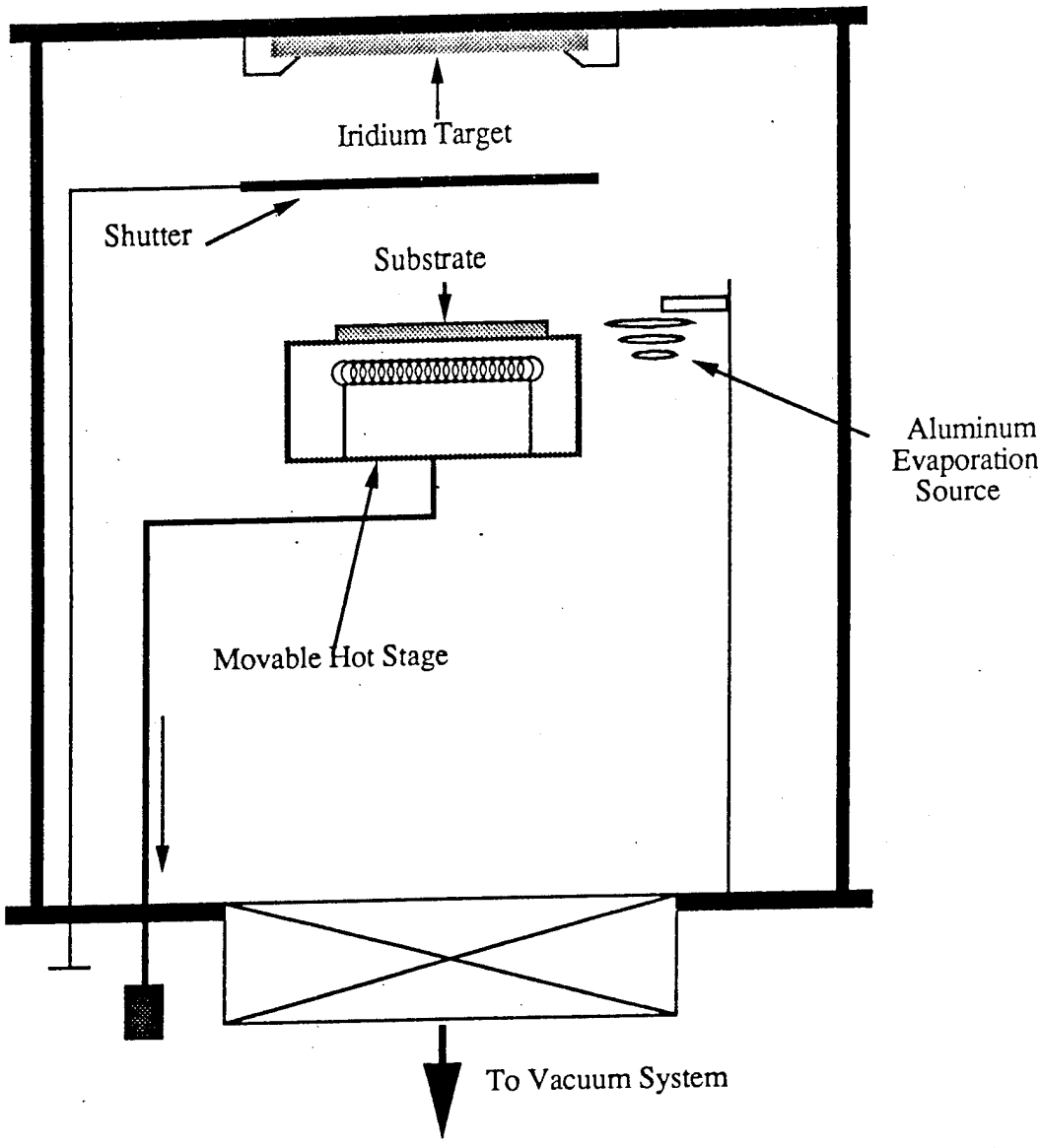

Figure 20. Schematic of the sputter/evaporation chamber.

Table 3 Deposition parameters and rates or Ir and Al.

Element	Method	Parameters	Rate (μm/min)
Ir	R.F. Sputtering	400 W 13.56 MHz 4 x 10^{-3} torr	0.1
Al	Thermal Evaporation	5 x 10^{-6} torr	0.2 - 0.5

Table 4 Ir-Al coating schemes.

	Scheme 1	Scheme 2	Scheme 3
No. of Layers	6	2	2
Order	Ir-Al-Ir-Al-Ir-Al	Ir-Al	Ir-Al
Initial Substrate Temp	700°C	700°C	700°C
Substrate Temp. for Subsequent Layers(C)	400°C	400°C	400°C
Thickness Ir (μm)	1.0	3.0	6.0
Thickness Al (μm)	1.2	4.0	8.0

4.3 Characterization of Coating

Figure 21 is an SEM image of a cross section from the as deposited six layer Ir-Al coating. In the as deposited condition, the coating was adherent to the substrate and showed no signs or cracking or spalling. An X-ray analysis of the film showed it to be Ir and Al, indicating that no solid state reaction had occurred between the two metals during the deposition process, see Figure 22. After heating the coating for 1 hour at 1000°C in argon, the coating cracked and exposed the SiC substrate. This implies that the coefficient of thermal expansion of the coating was greater than that of SiC substrate (3.9 - 4.8 x10^{-6} °C^{-1}), see Figure 23. X-ray analysis of the heat treated coating showed that both IrAl and Ir were present, indicating that insufficient amounts of Al were deposited, see Figure 22. In some regions, what were the top four unreacted layers buckeled, leaving only the cracked, first layer adherent to the substrate, see Figures 24 (a) and (b). Closer examination of Figure 21 showed that the Ir layers which were deposited at 400°C were porous. This allowed the Al to infiltrate the Ir layer during the heat leaving a void between the Ir layers. As the Ir and Al reacted to produce IrAl the

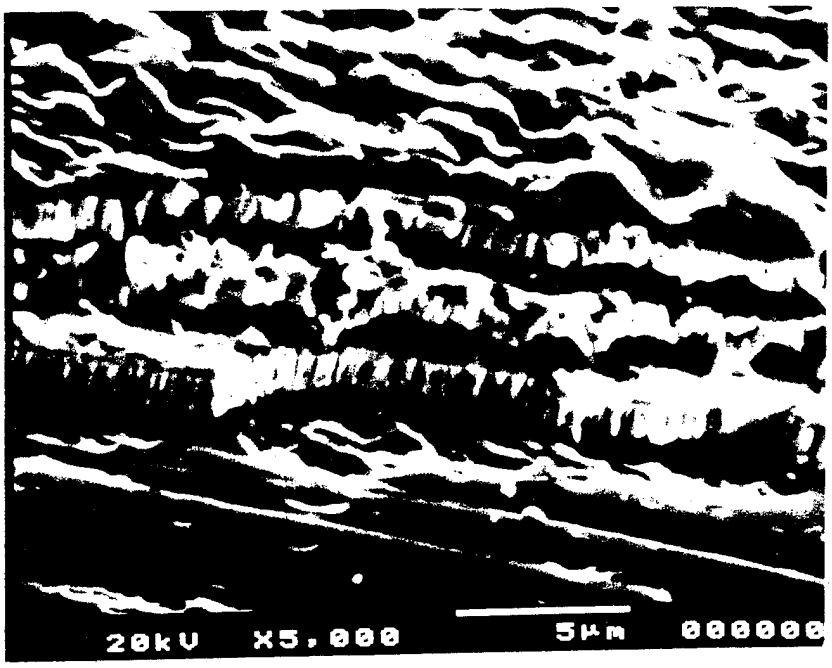

Figure 21. SEM image of the as deposited six layer Ir-Al coating.

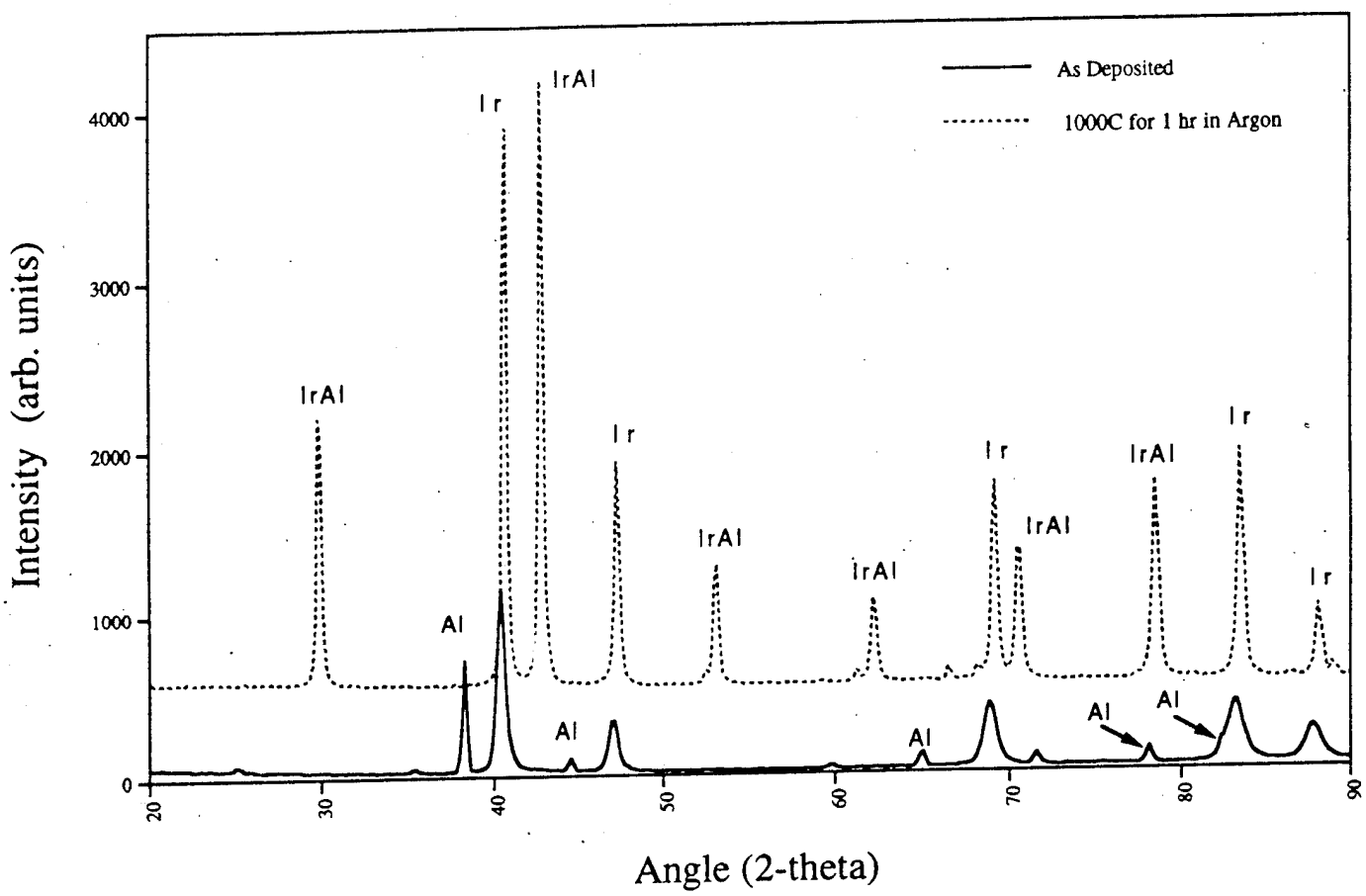

Figure 22. X-ray analysis of the six layer coating in both the as deposited and as reacted conditions.

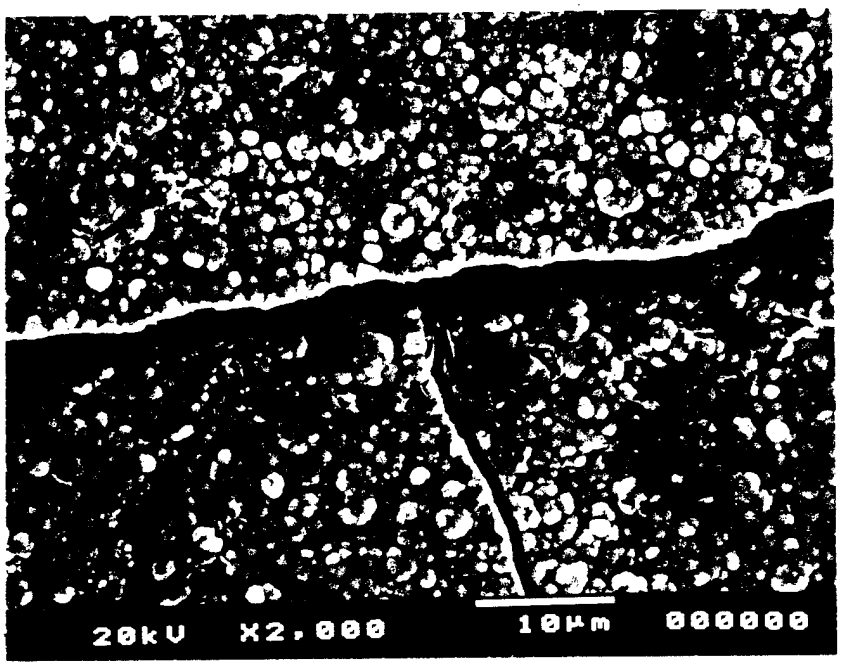

Figure 23. SEM image of the heat treated (1000°C for 1 hour in argon) six layer Ir-Al coating showing cracking.

a

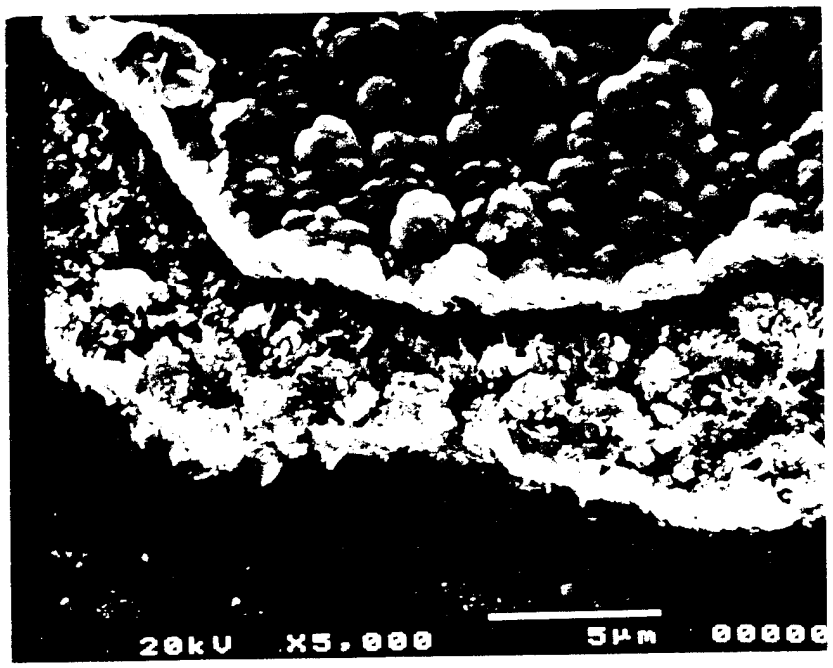

b

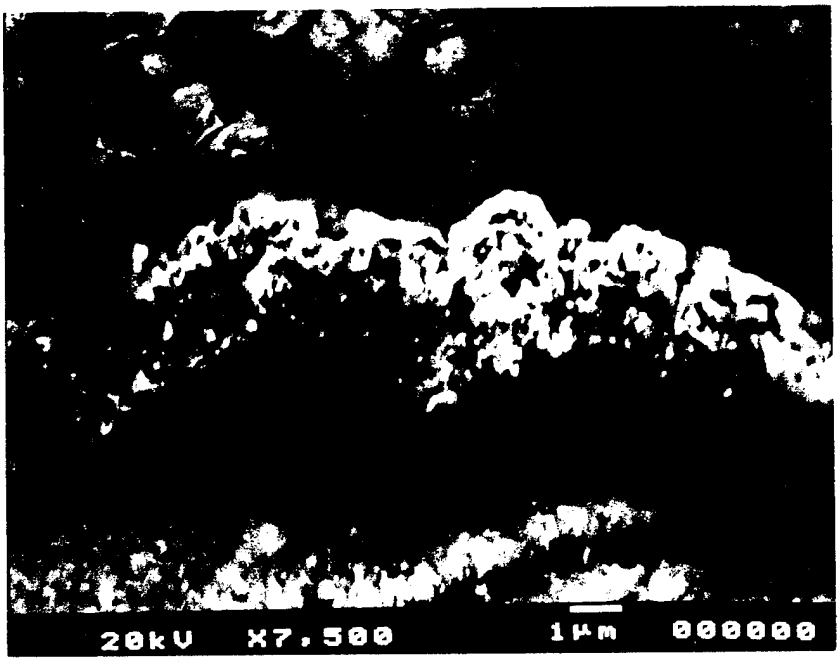

Figure 24. SEM image of the heat treated six layer Ir-Al coating showing (a)delamination, and (b) buckeling.

individual Ir layers buckeled. Preliminary differential scanning calorimetry (DSC) performed on the six layer coating, indicated that the reaction between Ir and Al begins at approximately 648°C and reaches a maximum at approximately 661°C (Al melts at 660°C). In addition, the reaction was found to be exothermic, see Figure 25.

In order to prevent debonding between the subsequent IrAl layers, a two layer coating was attempted which was comprised of a single Ir and a single Al layer, see Figures 26 (a) and (b). Here again, X-ray analysis indicated only Ir and Al were present, confirming no solid state reaction occurred during deposition, see Figure 27. Upon heating to 700°C in vacuum, the DSC data indicated that the reaction was completed by 680°C, the coating on the polished SiC showed evidence of massive cracking, Figure 28, while the coating on the as deposited SiC-C FGC exhibited a "fish mouth" like fracture along the facets of the SiC crystals, see Figures 29 (a)and (b). X-ray analysis of the as reacted coating indicated that all the Al and most of the Ir had reacted to form IrAl, see Figure 27. The scan also indicated that the Ir had reacted with the SiC substrate, producing $IrSi_3$ and graphite. Examination of a cross section of the reacted coating, Figure 29(b), showed both the reaction zone between the Ir and Al and between the Ir and SiC. Upon exposing the reacted IrAl coated SiC-C FGC to the same high temperature, oxygen rich, hydrogen torch used to on the bare SiC-C FGC, Figures 30 (a) and (b), the surface morphology remained relatively unchanged. The X-ray analysis of this surface indicated that the IrAl coating had formed an alumina layer on the surface, see Figure 27. However, due to the poor coating quality it was assumed that any additional oxidation protection provided by the coating would be marginal.

The final coating scheme called for thick layers of Ir and Al, 6μm and 8μm, respectively. Unfortunately, the coefficient of thermal expansion mismatch between the Ir and SiC caused the coating to crack and peel off the substrate during the deposition of Al. Figure 30 shows a cross section of the as deposited, thick Ir layer with a thin overlayer of Al. Due to poor adhesion of the Ir layer further evaluation of the thick coating scheme was terminated.

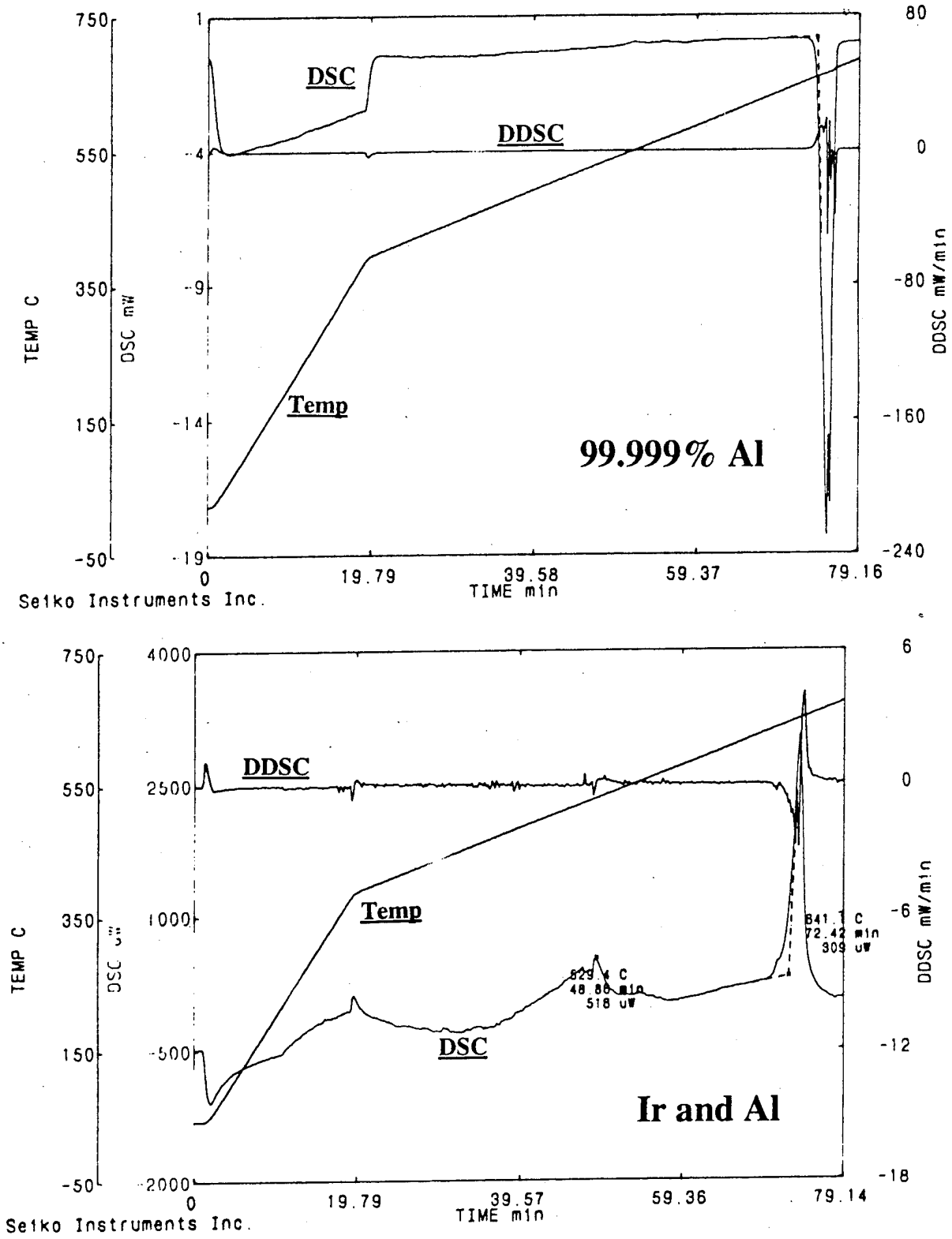

Figure 25. DSC scan from pure Al sample and six layer Ir-Al coating.

a

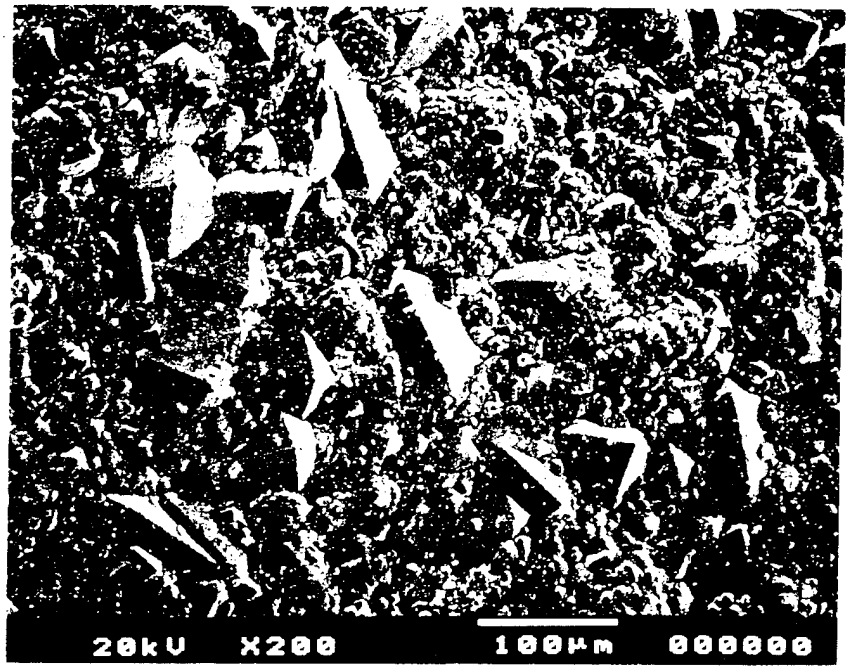

b

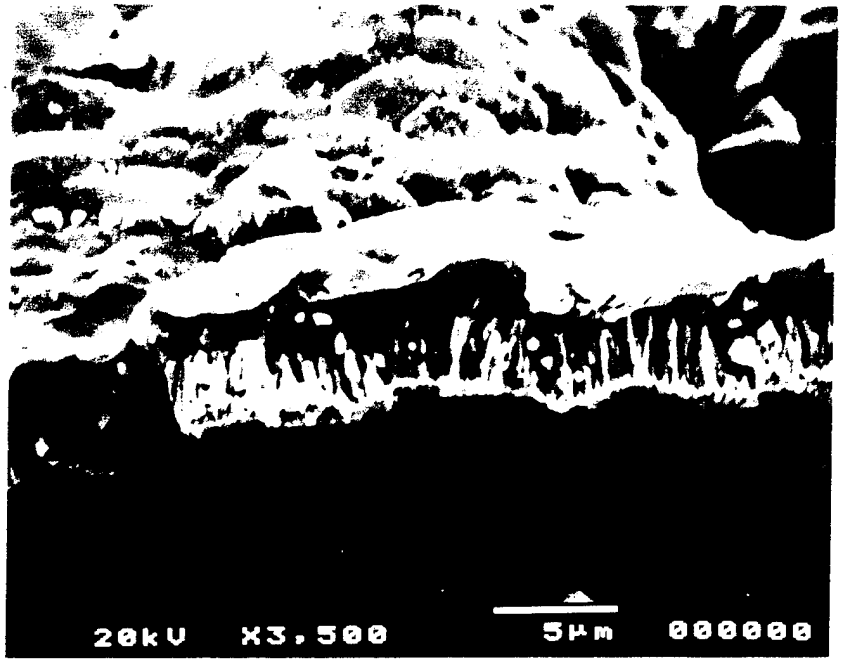

Figure 26. SEM images showing a top view (a), and a cross section (b), of the thin, as deposited, two layer Ir-Al coating.

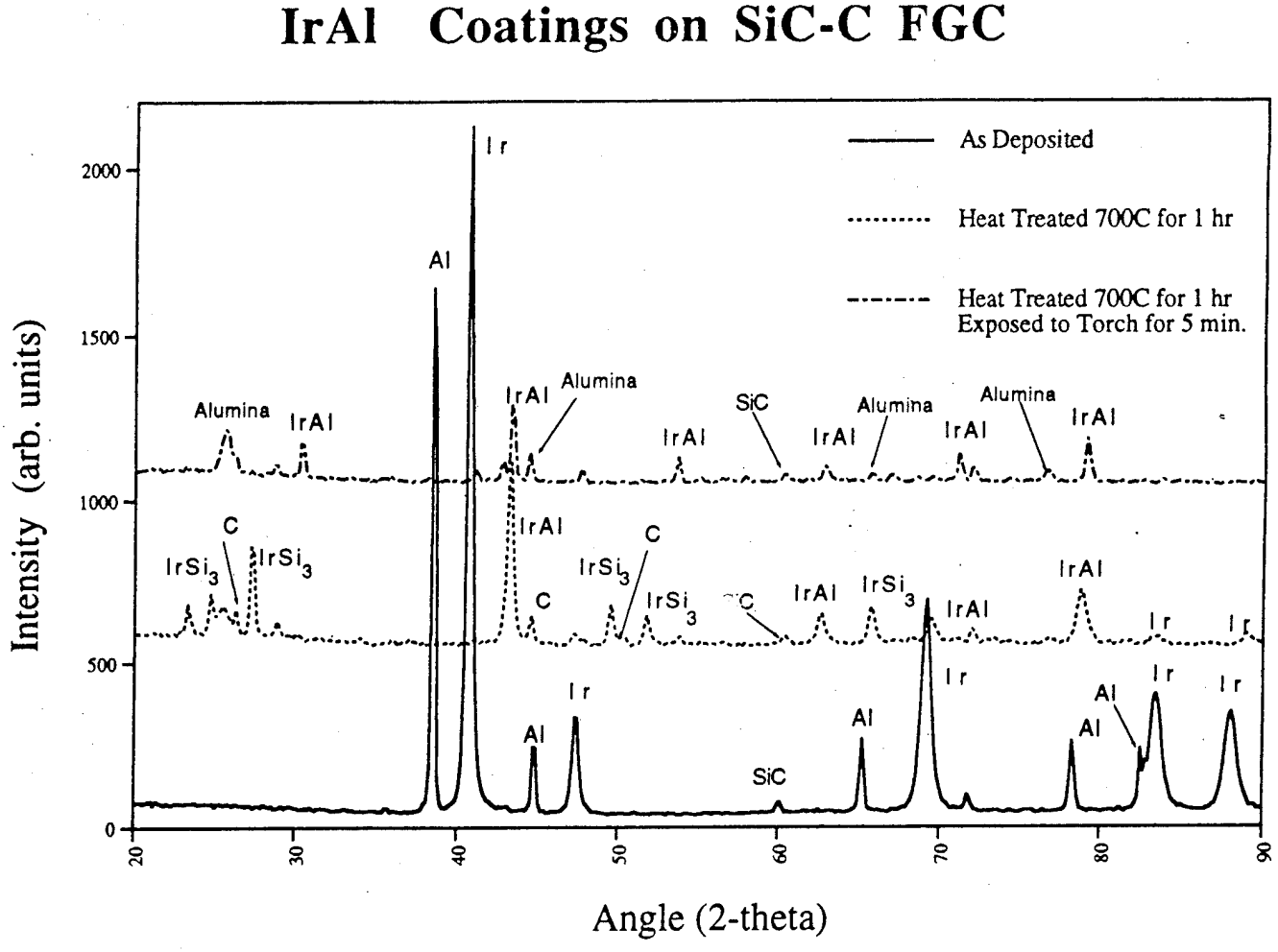

Figure 27. X-ray analysis of the two layer coating in the as deposited, as heat treated, and as oxidized conditions.

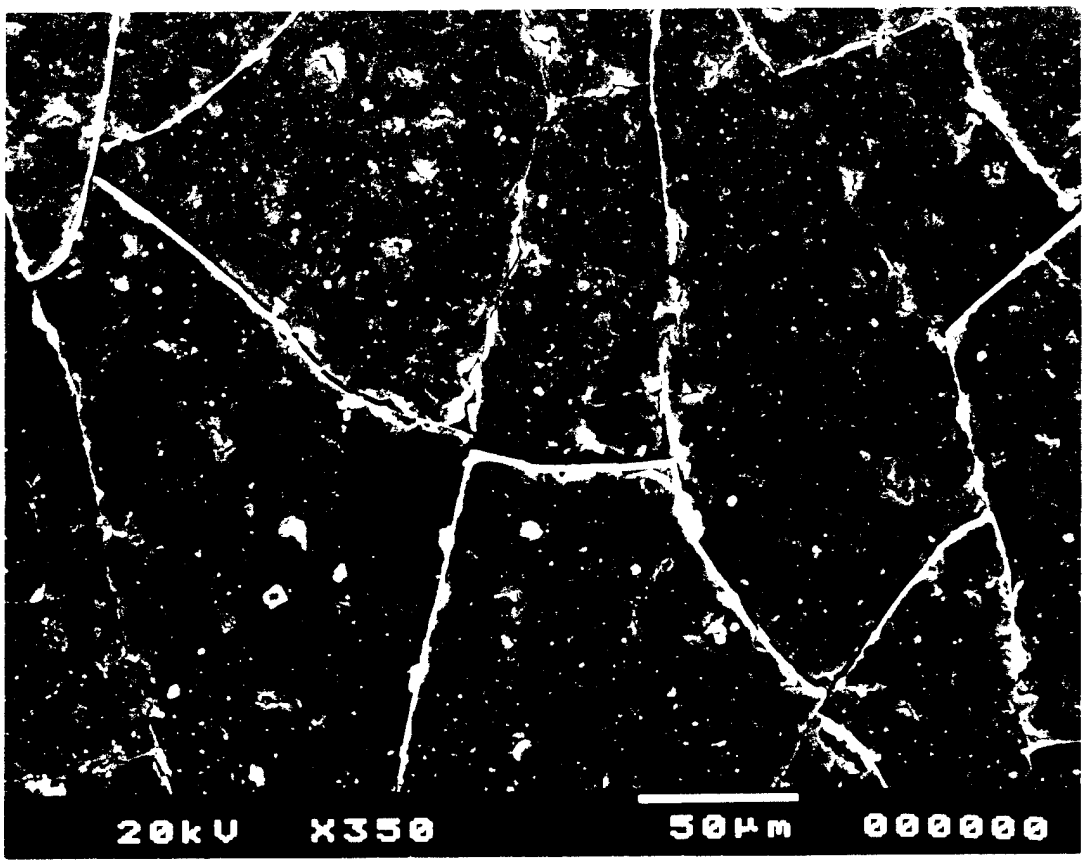

Figure 28. SEM image of cracking of the two layer heat treated IrAl coating on polished β-SiC.

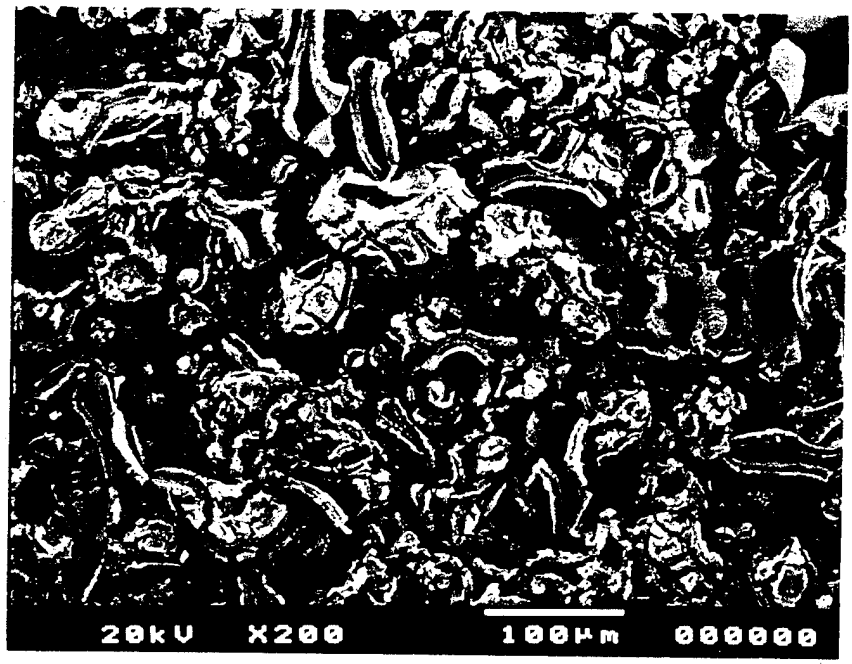

Figure 29. SEM image of cracking over the facets of two layer heat treated IrAl coating on the as deposited SiC-C FGC.

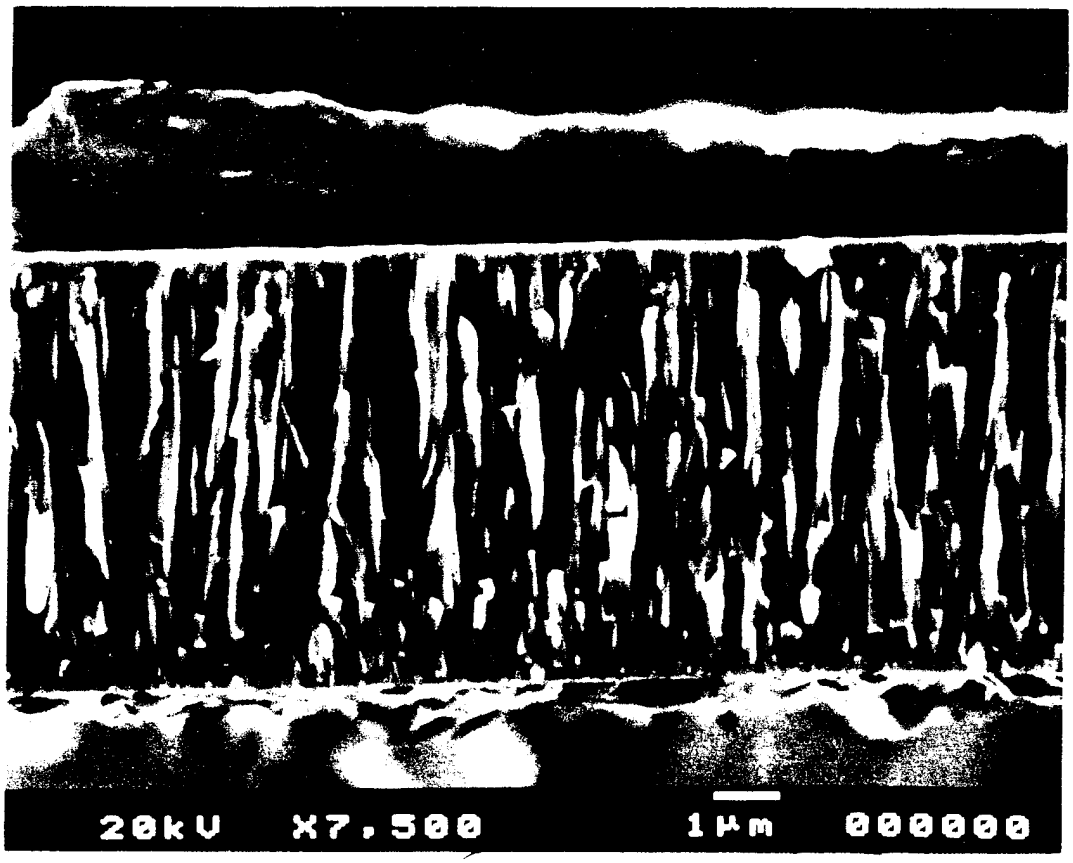

Figure 30. SEM image of the as deposited 6µm thick Ir layer.

5.0 Conclusions

1.) SiC-C FGCs can be produced with any desired compositional profile by alter the Si to C ratio in the reaction gas stream.

2.) SiC-C FGCs will remain adherent to a graphite substrate through thermal cycling between 20C and 2000C. In addition, the same coatings show no signs of cracking or spalling upon rapid exposure to high temperature oxidizing environments.

3.) By employing a conical induction coil in conjunction with a conventional cold walled CVD reactor, a conductive substrate can be simultaneously levitated and completely encapsulated with a continuous CVD coating. Additionally, the surface morphology of that coating can be controlled by altering the reactant gas flow rate and the chamber pressure.

4.) An IrAl coating can be produced by alternately depositing layers of Ir and Al, followed by a subsequent heat treatment to 700°C in vacuum or inert atmosphere.

5.) Ir reacts with SiC to form $IrSi_3$ and graphite at temperatures as low as 700°C.

6.) Due the poor coating quality caused by the low temperature reaction between Ir and SiC and the coefficient of thermal expansion mismatch between IrAl and SiC, the added expense of depositing an IrAl protective coating onto a SiC-C FGC is not out weighed by an in increase in oxidation resistance.

6.0 Future Work

Future work will focus on developing an auger electron spectroscopy (AES) technique which can be used to quantitatively analyze the ratio of SiC to C based on the AES line shape. Additionally, characterization of the LCVD technique will continue and be expanded to include the deposition of TiC, and FGCs of SiC-C and SiC-TiC. The interactions between the IrAl coating and SiC, and the IrAl coating and air will be further analyzed using differential scanning calorimetery and auger analysis. Considerable attention will be given to the SiC and IrAl interface and the formation of $IrSi_3$.

In order to improve the adhesion of IrAl to SiC, the coefficient of thermal expansion of IrAl first needs to be determined. After which, a coating scheme can be developed to reduce the CTE mismatch between the coatings.

7.0 References

Choi, Byung Jin and Dai Ryong Kim. "Growth of Silicon Carbide by Chemical Vapour Deposition", *J. Mat. Sci. Let.*, vol. 10, 1991.

Clift, W.M, McCarty, K.F., Boehme, D.R, "Deposition and Analysis of Ir-Al Coatings for Oxidation Protection of Carbon Materials at High Temperature", *Surface and Coatings Technology*, 42, 1990, 29-40

Gambling, W.A., Matsumara, H., and Ragdale, C.M. (1979) *Electron. Lett.*, 15, 474.

Hirai, T. and Sasaki, M. (1991) *JSME International Journal*, Series I, 34, 2, 123.

Lee, K.N., Worrell, W.L., "The Oxidation of Iridium-Aluminum and Iridium-Hafnium Intermetallics at Temperatures above 1550C", *Oxidation of Metals*, 32, Nos. 5/6, 1989, 357-369.

Muck, O., German Pat. 422004, October 30, 1923

Muramatsu, K.,Kawasaki, A., Taya, M. and Watanabe, R. (1990) *Proc. 1st Intl. Symp. Functionally Gradient Materials,* Edited by M. Yamanouchi, K. Koizumi, T. Hirai and I. Shiota, Sendai, Japan., p. 53.

Parretta, A., G. Guinta, E. Cappelli, V. Adoncecchi, and V. Vittori. "Influence of Substrate and Process Parameters on the Properties of CVD-SiC", *Mat. Res. Soc. Symp. Proc.*, 168, 1990.

Parretta, A., A. Camanzi, G. Giunta, and A. Mazzarano. "Morphological Aspects of Silicon Carbide Chemically Vapour-deposited on Graphite", *J. Mat. Sci.*, 26, 1991.

Pierson, Hugh O. Handbook of Chemical Vapor Deposition (CVD): Principles, Technology, and Applications. New Jersey: Noyes, 1992.

Sasaki, M and Hirai, T. (1991) *J. Ceram. Soc. of Japan*, The Centennial Memorial Issue, 99, 10.

Sasaki, M., Hirai, T., and Takahashi, H. (1990) *J. Jpn. Soc. Powder and Powder Mat.*, 37, 966.

Taya, M., Hayashi, S, Kobayashi, A.S. and Yoon, H.S. (1990) *J. Ame. Ceram. Soc.*, 73, 1382.

Taya, M., Lulay, K.E., and Loyd, D.J. (1991a) *Acta Metall. Mater.*, 39(1), 73.

Taya, M., Muramatsu, K., Lloyd, D. J., and Watanabe, R. (1991b) *JSME Intl*, J. Ser. I, 34 (2), 198.

Wang, Y., Sasaki, T. Goto, T., Hirai,T., Journal of Materials Science, 25, 1990, 4607 - 4613

Wang, Y., M. Sasaki, T. Hirai. "Density and Microstructure of CVD SiC-C Nanocomposites", *J. Mat. Sci.*, 26, 1991.

Watanabe, R. (1993) Functionally Gradient Materials, Kogyo Chosakai, Tokyo, Japan.

Wei, G.C. and Becher, P.F. (1984) *J. Am. Ceram. Soc.*, 67(8), 571.

Publications and Presentations

Publications

M.R. Richards, A.C. Richards, M. Taya, F.S. Ohuchi, Thermo-Mechanical and Chemical Properties of SiC-C Functionally Gradient Coatings on Graphite and C/C Composites, Journal of Vacuum Science and Technology A: 41 st AVS National Symposium Conference Proceedings, Denver, CO , October 24-28, 1994 Vol. 13, No. 3, Part 1, pp196-1201, 1995

Presentations

Fabrication and Characterization of SiC-C Functionally Gradient Coatings, **M.R. Richards**, A.C. Richards, M. Taya, F.S. Ohuchi, 6 th Annual Pacific Northwest Symposium, Troutdale, OR, September 15 and 16, 1994

Thermo-Mechanical and Chemical Properties of SiC-C Functionally Gradient Coatings on Graphite and C/C Composites, **M.R. Richards**, A.C. Richards, M. Taya, F.S. Ohuchi, 41 st AVS National Symposium Conference Proceedings, Denver, CO, October 24-28, 1994

Fabrication and Characterization of IrAl Thin Films on SiC-C Functionally Gradient Coatings, **M.R. Richards**, M. Taya, F.S. Ohuchi, International Conference on Thin Films and Metallurgical Coatings, San Diego, CA, April 24-28, 1995

A New, Versatile Coating Technique: Levitation Chemical Vapor Deposition, **A.C. Richards**, F.S. Ohuchi, M. Taya, International Conference on Thin Films and Metallurgical Coatings, San Diego, CA, April 24-28, 1995